THE UNIVERSITY OF KANSAS
PALEONTOLOGICAL CONTRIBUTIONS

February 10, 1975 **Paper 74**

THE MICROSTRUCTURE OF THE CRINOID ENDOSKELETON[1]

DONALD B. MACURDA, JR. AND DAVID L. MEYER

The University of Michigan, Ann Arbor; Smithsonian Tropical Research Institute, Balboa, Panama

ABSTRACT

The microstructure of the crinoid endoskeleton is highly differentiated in Recent crinoids, reflecting types of tissue, the functions of the plates, and the autecology of the animals. Stem plates are interconnected by long ligament fibers that penetrate into the skeleton, producing a galleried structure. Both movable and immovable articulations exist; specialized projections stabilize the plates along a fulcral ridge in some synarthries. The cirri, attached to a nodal stem plate or a centrodorsal, have differentiated articular surfaces in which the greater development of ligaments in a dorsal (lower) position enhances their clasping power. Accessory nerve canals are present in some stem plates and penetrate the basals into the region of the axial organ. The basals and radials are pierced by intricate nerve canals that give rise to branches enclosed within the brachials.

Several types of articulations are found within the arms. The muscular articulation, divided into three parts, has galleried microstructure in two of these for the long ligament fibers that penetrate the skeleton, whereas muscle tissue does not and is reflected in a more disordered or labyrinthic microstructure. Many fulcral ridges show wear. Other arm articulations such as syzygies, synarthries, and symplexies have highly differentiated, three-dimensional surfaces. A pinnule articulates with the brachial on an asymmetrical muscular articulation. By having subsequent pinnular articulations articulate in a different plane and also modifying the fulcral ridges, great flexibility can be achieved in some pinnules. Peculiar lumina on the upper surfaces of some pinnulars remain uninterpreted. Analogous microstructures in fossil crinoids enhance their paleobiological interpretation.

INTRODUCTION

The endoskeleton of the modern echinoderm is a remarkable structure, which differs from that of other invertebrates. It is composed of a high-magnesium calcite and each plate behaves optically as a single crystal. Secreted within the mesoderm, the endoskeleton has a meshlike stereom that can also be seen in fossil echinoderms from as far back as the Cambrian. The stereom is formed from a series of rods or trabeculae which are cross-connected. The porosity of the stereom varies within different parts of a plate. The holes of the mesh are filled with tissues, some of which are ligaments.

The skeleton of a crinoid is composed of many different kinds of plates, each with different functions. Most have distinct canals within them which contain nerves and in some instances coelomic extensions. The porous nature of the skeleton has been observed by paleontologists (e.g., Strimple, 1972) and zoologists, but until the advent of the scanning electron microscope, it has not been possible to appreciate the three-

[1] Manuscript received February 26, 1974; revised manuscript received August 14, 1974.

dimensionality of the stereom or to interpret it functionally. Roux (1970, 1971, 1974) has applied the SEM to the interpretation of some of the stems of the Mesozoic, Cenozoic, and Recent members of the orders Millericrinida and Isocrinida, two of the seven orders of the Articulata. Four of the seven orders have living representatives, and this study is based upon nine modern genera from the orders Isocrinida, Comatulida, and Millericrinida as listed below:

Isocrinida
- *Endoxocrinus parrae* Gervais
- *Neocrinus blakei* (Carpenter)

Comatulida
- Comatulina
  - *Comactinia echinoptera* var. *meridionalis* (Agassiz and Agassiz)
  - *Comactinia echinoptera* var. *valida* (Hartlaub)
  - *Nemaster rubiginosa* (Pourtalès)
- Mariametrina
  - *Analcidometra armata* (Pourtalès)
- Thalassometrina
  - *Crinometra brevipinna* (Pourtalès)
- Macrophreatina
  - *Atelecrinus balanoides* Carpenter
  - *Ctenantedon kinziei* Meyer

Millericrinida
- *Democrinus* sp.

Four of the genera (*Analcidometra, Comactinia, Ctenantedon,* and *Nemaster*) are found at depths of 10 to 50 meters. The others generally occur at depths of a few hundred meters. The observation of similar structural patterns in the stereom in different orders which originated in the Triassic and Jurassic implies generalizations for the interpretation of the paleobiology of fossil Articulata and perhaps Paleozoic subclasses as well.

ACKNOWLEDGMENTS

This study was conducted in the Microprobe Laboratory, The University of Michigan, Dr. W. C. Bigelow, Director, with the able assistance of Larry Allard, Peggy Hollingsworth, and John Mardinly, to whom deep appreciation is expressed. Drs. G. Voss and T. Bayer, University of Miami, kindly made the Gerda and Pillsbury crinoid collections available to us. Drs. J. Bunt, D. Taylor, and Mr. C. Messing made many field opportunities available from the R/V *Columbus Iselin*. Appreciation is also expressed to Dr. L. Land, University of Texas, who made time available to us in the *Nekton Gamma* (NSF GA-35111), and the staff of the Discovery Bay Marine Laboratory, Jamaica. The manuscript was reviewed by Dr. A. Breimer, Vrije Universiteit, Amsterdam, and Dr. N. G. Lane, Indiana University. The research was supported by NSF grant GB-36439.

MICROSTRUCTURE OF THE CRINOID ENDOSKELETON

PROCEDURES

Direct observation of the shallow water genera (*Analcidometra, Comactinia, Ctenantedon,* and *Nemaster*) was effected with SCUBA during a two-year study of the zoogeography of West Indian crinoids. Observations of some of the deep water genera (*Democrinus* and *Endoxocrinus*) were made from the submersible *Nekton Gamma* off Jamaica (Macurda & Meyer, 1974). Shallow specimens were collected by us; deep specimens were obtained by the R/V *Gerda* and *Pillsbury,* University of Miami. Specimens studied were chloroxed and then individual plates mounted on aluminum stubs with Duco cement. All micrographs were taken with a Japan Electronic Optic Laboratory Model JSM-U3 scanning electron microscope located in the Microprobe Laboratory, College of Engineering, The University of Michigan. Specimens were coated with 250-300 angstroms of gold and photographed at 15 KV with Polaroid PN type 55 film. Over 800 micrographs, many of which were stereo pairs (made by tilting the stage 7° and then recentering) were used to study the skeletal microstructure. Smaller pore diameters were measured directly from micrographs taken at or near a vertical orientation to the plate; accuracy is estimated at ± 5 percent. Pore area was determined by point counting about 100 points at intervals of 2.5 mm along the two long diagonals

of a micrograph and converting the ratio of pores to skeletal rods to a percentage, rounded to the nearest tenth.

STEM

The stem plates of the Isocrinida as seen in *Endoxocrinus* or *Neocrinus* are cylindrical to pentagonal, with a central lumen. There are two types, the nodals which bear cirri (Pl. 1,*2*) and the more numerous internodals (Pl. 1,*1*). The internodals have a pentameral petaloid pattern on the upper and lower surfaces (articula; terminology follows Moore *et al.,* 1968). The areola forms the center of these pentameral patterns and the crenulae border them, forming the petalodium (Pl. 1,*1*). Long ligament fibers occupy the pores (interstices) of the areola. The position of the ligament fibers is clearly indicated in the endoskeleton, because all of the pores are aligned internally, producing a galleried pattern (Pl. 1,*3,5,6*; Pl. 2,*3*). This microstructure characterizes the presence of ligament fibers in both the stem and brachials. Within the stem, ligaments are also present in the crenellae. The culmina are strongly elevated above the surface of the plate (Pl. 2,*1,2*) and provide lateral resistance to shearing. The stiffness provided by the combination of the long ligament fibers and culmina (which interlock with the crenellae, producing a symplexy) provide an effective structure that keeps the crown of a crinoid elevated even in moderate currents (Meyer, 1971; Macurda & Meyer, 1974).

The areola is slightly concave and its central portion lies slightly below the level of the plate around the lumen. The pores occupy about 50 percent of the surface area and show some rectilinear regularity in their arrangement. They are circular to subelliptical and vary from 0.010 to 0.023 mm (see "Procedures") in diameter in *Endoxocrinus*. Internally the galleries are very straight and well developed.

The upper surface of the culmina and the lower surface of the crenellae lie at nearly equal levels above and below the areola. The pores also occupy about 50 percent of the surface area (= pore area hereafter) of the culmina and crenellae in *Endoxocrinus*. The stereom of the culmina is strongly galleried internally, but that of the crenellae is less regular. Culminal pores are circular to ovoid and vary from 0.012 to 0.025 mm in diameter. The sides of the culmina are buttressed by long straight vertical ridges and the surface pore area is reduced. Diameter of the crenellar pores varies from 0.015 to 0.027 mm.

The lumen, whose diameter is 0.244 mm in *Endoxocrinus,* is surrounded on the surface by a pentagonal area (perilumen, see Pl. 1,*1*) in which the pore area of the stereom is reduced to about 20 percent. The diameter of the pores is reduced (0.007 to 0.009 mm) compared to the areola or crenula. The surface of the perilumen has a worn, fractured appearance. Stresses generated between adjacent stem plates or by greater contraction on one side of the stem than another are apparently localized here, resulting in wearing of the stem plate.

Some larger pores (up to 0.038 mm) are found in the radial parts of the stem plate (Pl. 1,*1,2*). They occur only very rarely in the outer part of the perilumen; they begin immediately beyond it. Their spacing is regular in some radii, but irregular in others. They do not occur in the petaloid parts of the areola, but occur in the parts of the petalodium adjacent to the areola. They become less common abcentrally. They are continuous through several internodals, but are not as well developed abcentrally on the synostosial (distal) facet of a nodal of *Endoxocrinus* as they are in *Neocrinus*. They are also found penetrating the basals on the articulum on their lower surface in both *Endoxocrinus* (see Pl. 7,*1,2*) and *Neocrinus*. They may serve as accessory canals for nerves.

In contrast to the highly sculptured surface of most internodals, the distal surface of each nodal (and proximal surface of the proximal internodal of a noditaxis) is almost smooth in *Endoxocrinus* and *Neocrinus* (Pl. 1,*2*). This synostosis lacks a perilumen and the only ornaments are five very low radially sited parabolic ridges, which open abcentrally, and three or four very low marginal ridges and grooves (Pl. 3,*1*). The lumen of the synostosis is narrower in diameter (0.200 mm) than that of the symplexy in *Endoxocrinus*. Long daggerlike extensions of the stereom may project 0.056 mm into the lumen (Pl. 1,*4*). These are found only for a slight distance above and below the synostosis; thereafter the lumen is a straight, uninterrupted cylinder. The stereom of the parabolic ridges is

denser than that of the surrounding areas. The stereom within the parabolic ridge is irregular in appearance, has a pore area of 20 to 30 percent, and ovoid pores with diameters of 0.004 to 0.018 mm. The stereom in an interradial position between the parabolas (corresponding to the areola) has a pore area of 50 percent, and is galleried internally. The pores vary from 0.004 to 0.012 mm in diameter and are, therefore, about half the size of those in the areola (0.010 to 0.023 mm). The ligament fibers are thus apparently thinner; the pores also lack the rectilinear pattern found in the areola. Ligament fibers are distributed over most of the surface of the synostosis, including the area immediately adjacent to the lumen where the pore area remains as high as the area between the parabolas. However, the lack of crenulae makes this suture much weaker and the stem usually breaks along a synostosis when subjected to stress or comes apart there first after death.

In some synostoses, the area within each parabola is deepened to form a radial groove which extends to the periphery, but it does not extend to the lumen (Pl. 3,*1*). If the synostosial surface is on a nodal, the groove leads outward to a cirral facet. The size of the pores of the stereom within the radial grooves is larger than those of the stereom external to the radial grooves.

The most distal columnal of the column is a nodal. Its distal surface shows the five parabolic areas corresponding to the ridges, but the porosity of the entire surface is greatly reduced, the lumen is closed, and there are none of the larger pores that are present on synostosial and symplexial surfaces.

The similarity of the microstructure described above for *Endoxocrinus* and *Neocrinus* suggests the features are common in living Isocrinida.

In his study of fossil stems of the Isocrinida, Roux (1970, 1971) distinguished two types of stereom. His type alpha corresponds to that seen in the petaloid areola and his type beta was characteristic of the petalodium and other abcentral parts of the articulum. He demonstrated the presence of types alpha and beta in four Mesozoic genera (*Balanocrinus, Isocrinus, Extracrinus,* and *Pentacrinus*). The measurement he used to indicate the dimensions of the stereom was the sum of the diameter of a pore plus the width of its adjacent bar. The resulting figures are thus larger than those previously given for *Endoxocrinus,* but the range is quite comparable. The rectilinear pattern seen in Roux's (1970) illustrations of the areola of the Jurassic genus *Balanocrinus* and the relevant dimensions indicate evolutionary stability in the placement and function of the ligaments in the stems of the Isocrinida. Roux (1970, 1974) suggested there might be muscular tissue in the stem of the Isocrinida, but the differences seen in the microstructure of the stereom of the ligament and muscle fossae of the brachials of Recent crinoids do not appear to support this.

In contrast to the stems of the Isocrinida, the stem of a modern Millericrinida such as *Democrinus* has well-developed synarthrial articulations on the proximal and distal surfaces of each mature columnal (Pl. 2,*4*). The articulum is elliptical in cross section and a massive fulcral ridge bisects the long axis (except at the center where the elliptical lumen, longest diameter 0.113 mm, is present), separating the two bifascial ligament fields. The longer axes of the articula are at right angles to one another on the proximal and distal faces of a columnal. The fulcral ridges and the immediately adjacent knobs are the highest and lowest points on the columnal (Pl. 2,*6*). The ligaments on either side in the two deep fossae thus can slightly flex the stem at each articulation. The alternate orientations of the fulcral ridges allow flexure in any direction. This type of stem is effective in holding the crown above the substrate in moderate currents and no portion of the stem above the root is in contact with the substrate (Macurda & Meyer, 1974). Each synarthry is quite taut in specimens preserved in alcohol and if stressed and released, quickly springs back to position.

The fulcral ridge is a massive, nonporous structure. It has a series of very narrow grooves (0.0013 mm), which cross it at right angles and are spaced 0.007 to 0.011 mm apart (Pl. 2,*6,7*). Their function is unknown. A single line of regular, larger pores, 0.016-0.017 mm in diameter, parallel either side of the fulcral ridge from the lumen to the edges of the articulum. They are alternately offset on either side of the ridge. These specialized pores are smaller than those in the Isocrinida, but may have served a similar function. There is a rounded knob between each

set of pores that stands elevated above the fulcral ridge. These knobs are almost the same width (0.016 mm) as the diameter of the larger pores and are alternately offset from one another on opposite sides of the fulcral ridge. Given the height of these knobs above the fulcral ridge, the opposing columnal would have rested on them and not on the fulcral ridge unless the knobs on the opposing columnal fit into the space represented by the larger pore. Then the opposing columnals would have been in contact along the fulcral ridge and the knobs would have served to keep the opposing columnals in contact along the ridge and to prevent any lateral shearing upon flexure (Pl. 2,*5*). The similarity in dimensions of the knobs and larger pores may support this hypothesis.

The stereom of the articulum is galleried, both within the bifascial fossae and the flat area adjacent to the fulcral ridge; groups of the pores show a rectilinear pattern. Because of the depth of the fossae, some ligament fibers extend unsupported over a very long distance. The pores are ovoid and 0.007 to 0.015 mm in diameter. Pore area is about 40 percent. The pores on the exposed exterior of the columnal are of similar size (0.007-0.014 mm), but much less regular in their distribution, and pore area is only 20 percent.

Synarthrial articulations are found throughout most of the stem of *Democrinus*. New plates, however, are added below the calyx. When first formed, these disc-shaped plates form a synostosis. Growth elongates the columnals and they are modified to form synarthies (see also Breimer, in press).

Roux (1970) examined the microstructure of the stem of the Jurassic genus *Apiocrinites,* a genus of the Millericrinida. He found only one type of stereom within the stem and noted a resemblance to his type alpha (= galleried) of the Isocrinida.

CIRRI

In modern crinoids, cirri are found attached to the nodal plates of the stem of the Isocrinida and the centrodorsal of the Comatulida; they are lacking in the Millericrinida and Cyrtocrinida. The cirrals are usually short, cylindrical plates with ligamentary articulations between adjacent plates. They clasp onto the substrate or objects and thus secure the crinoid. In the Isocrinida, those attached to dististele nodals may be partly buried in the sediment, functioning as a root or prop (Macurda & Meyer, 1974). The cirri of the Comatulida may cling to an object very tenaciously and it may be necessary to free them almost individually or else they will break first. They will also act to resecure a crinoid fairly rapidly if displaced.

The nodals of the Isocrinida *Endoxocrinus* bear five nodicirral articula. The facets are depressed within the nodal and are elliptical in outline, the longer axis paralleling the plane of the nodal articulum (Pl. 3,*1,2*). The lower half of the facet is more depressed, thus imparting a downward slant to the cirri. An ovoid lumen, 0.12 mm in diameter, is present in the center; it is a lateral extension of the axial canal of the columnals into the cirri. Two knobs on either side of the lumen separate the upper and lower ligament fossae. The stereom of the upper and lower fossae is galleried, but does not show any rectilinear patterns. The pores are 0.009 to 0.016 mm in diameter; pore area is nearly 40 percent. The stereom on the surface (latus) of the nodal laterally adjacent to the nodicirral facet shows some vertical linearity of the pores; pore area is 20 percent.

The distal articulum of an *Endoxocrinus* cirral has a raised border, which slightly overlaps the proximal face of the adjacent cirral (Pl. 3,*3*). This rim has small spines (0.02 mm), which project distally. The exterior surface of the cirral is dense. The surface pore area is less than 10 percent and the pores are small, 0.004-0.006 mm. They show some linearity in their arrangement on the upper and lower surface of a cirral. A lumen (diameter 0.10 mm) pierces the cirral slightly above center. There is an ovoid raised area in the articulum immediately above the lumen; it has a concave center (Pl. 3,*4*). The stereom of the rim of the raised area is denser and has a lower pore area; the stereom of the concave center shows a typical galleried structure with pores having a diameter of 0.012-0.018 mm. Two raised areas occur lateral to the lumen on the proximal end of a cirral and fit into corresponding depressions on a distal face.

Ligaments are well developed on the cirral articulum. The most regular development of the galleried structure is found in the lower half of

the articulum where the pores are more regularly arranged and there are fewer smaller ones (diameter 0.009-0.018 mm). Pore area is 50 percent. Pores in the upper part of the articulum are more variable in size, being 0.013-0.017 mm in diameter nearer the raised area in the upper part of the articulum and 0.009-0.013 mm peripherally. The pores are galleried; pore area is about 50 percent. The cirral articulum is a ligamentary articulation. Each articulation has limited flexure in a vertical plane. The raised area with the denser stereom above the lumen would appear to have a limited fulcral function as would the raised areas laterally adjacent to the lumen on proximal facets. The primary function of a cirrus is to hold on for a prolonged period of time and this is effected by being bent in toward the stem. The more regular development of the stereom in the lower part of the cirral articulum reflects well-developed ligaments that effect this. The development of ligaments in the upper part allows the cirrus to be repositioned and the ligaments in the concave area within the elevated area may be instrumental in this.

In the Comatulida, the cirri are attached directly to the centrodorsal. In *Analcidometra,* these facets cover much of the lateral sides of the centrodorsal (Pl. 5,*2*). The facets are slightly depressed internally; their center is pierced by an elliptical lumen. There are low, raised areas on either side of the facet, which divide it into upper and lower fossae. The facets on the conical centrodorsal of *Atelecrinus* are quite different (Pl. 4,*1,2*; 5,*6*). They are arrayed in columns; each facet is taller than it is wide. They are deeply depressed and pierced by a central lumen (longer diameter, 0.118 mm). The fossae above and below the lumen are funnel-shaped; the lower is larger. The stereom is irregular in appearance and no gallery structure is evident. Pore area is near 30 percent; pores are irregular in shape and 0.002 to 0.005 mm in diameter. Pore diameter between the fossae and lumen is higher. Two large mesa-like elevations are present on either side of the lumen. They are about equal in size to the fossae and slope inward and upward. The surface stereom is denser than that of the plate outside the facet where pore area is 30 percent and pore diameter 0.006-0.010 mm. Thus, in contrast to the usual appearance, pore diameter of the stereom is larger on the free exterior rather than within the facet. The fossae are much more clearly delineated and separated than in other cirral facets. The structure of the stereom is not that seen in usual ligamentary fossae. Its functional significance is unknown, but it may account for the ease with which the cirri of *Atelecrinus* are broken off and may be the reason they are seldom attached to dredged specimens. The proximal cirral (Pl. 4,*3,4*) clearly shows the differentiation of the ligament fossae and its surface is a counterpart to that of the cirral facet.

The lumen of the cirral articulum of *Analcidometra* is located two-thirds of the distance to the upper edge (Pl. 3,*5*; 4,*5,6*). It is ovoid with a flat floor; its greatest dimension is 0.05 mm. Two knobs with denser stereom border it laterally on proximal articulata and fit into corresponding depressions on distal articula; some have apparent signs of wear. The lumen and knobs separate a small upper fossa from a well-developed concave lower fossa that occupies about two-thirds of the total area of the articulum. It has a well-developed gallery structure with a pore area of 50 percent. Pores are ovoid to subpolygonal without any linear pattern; pore diameter is 0.004-0.007 mm. Gallery structure is also present in the upper fossa but its area is one-quarter to one-third that of the lower fossa. Thus, as in *Endoxocrinus,* the majority of the ligaments are developed in the lower part of the articulum. A series of larger than normal pores forms a border to the lower fossa and knobbed area (and in some instances the upper fossa) in the cirri of *Analcidometra.*

The cirral articulum of *Ctenantedon* (Pl. 3,*6,7*) shows a similar pattern to that of *Analcidometra.* The cirrals are long and spindly; they are widest at the facet. Pore area along the shank is low. The elliptical cirral lumen is 0.057 mm in diameter and a massive arcuate ridge above the lumen on a distal articulum serves a limited fulcral function. It is densest immediately adjacent to the lumen. There is an elevated area below the lumen, but its stereom does not have an increased density. The upper fossa is again the smaller of the two; the stereom of both fossae shows a regular galleried structure. Pore area in the lower fossa is about 50 percent and the pore diameter is 0.004 to 0.006 mm except in the regions adjacent to the knobs, where

it increases to 0.009 mm. A ring of larger pores again border the articulum. The asymmetry of the cirral articulum enhances the clasping function of the cirri; contraction of the lower ligaments causes them to bend inward. Cirral spines probably also aid in a firm fixation to hard substrates.

CENTRODORSAL

The centrodorsal plate of the Comatulida is one of the largest plates found in the animal. Breimer (in press) has noted that ontogenetically it is the modified topmost columnal of the juvenile pentacrinoid stalk. The plate is hemispherical or conical (Pl. 5,*1,2,6*). Its lateral surfaces bear cirral facets; these may also be present on the dorsal surface, which is otherwise smooth. The upper surface is in contact with the basals (very rare), basal rays (*see* Pl. 8,*1,2*), and radials. The ventral surface has a cavity in which the chambered organ and main aboral nerve center are found (Pl. 5,*1*). In *Analcidometra* the lumen of each cirral facet can be seen passing through the centrodorsal into the cavity. The stereom within the cavity is irregular and has a pore area of about 30 percent (Pl. 5,*3*). Pores are ovoid with a diameter of 0.005-0.007 mm. The pore area of the ventral surface that is in contact with the radials is the same, but pore diameter is larger (0.006-0.014 mm). In *Nemaster,* the pore area of the stereom in the center of the cavity (Pl. 5,*4*) is only slightly higher than that of *Analcidometra,* but the pore diameter is much more variable (0.007-0.058 mm). The larger pores, which are relatively few in number, may represent nerve passages into the centrodorsal. Grooves for the basal rays are visible on the ventral surface of the centrodorsal. Pore area within the grooves is 50 percent; pores are ovoid and 0.011-0.020 mm in diameter. Pore area outside the grooves is 40 percent and the diameter of the ovoid pores is more variable (0.007-0.023 mm). The stereom is irregular in appearance. The suture between the centrodorsal and radials in *Analcidometra* and *Nemaster* is by definition a synostosis.

The cavity within the conical centrodorsal of *Atelecrinus* (Pl. 5,*5,6*) is much larger than that of *Analcidometra* or *Nemaster*. The ventral surface of the plate has five peripheral elevated buttresses with five low areas in between (Pl. 6,*1,2*). The buttresses are interradial in position and mark the center of a basal. The ventral surface of each buttress is highly differentiated. Two lateral triangular areas display prominent gallery structure, whereas a central triangular area, which may be slightly depressed medially, has a very lacy open stereom, the function of which is unknown. The pores are galleried and large (up to 0.04 mm) and pore area is between 60 and 70 percent. Pore area in the lateral triangular areas is somewhat lower and pore diameter smaller. A line of slightly larger pores forms an outer border to the buttress. The galleried structure of each buttress is reflected on the exterior by a triangular-shaped area in which vertical ribs are prominent. The depressed areas between the buttresses also have gallery structure. It is also evident on the internal walls of the centrodorsal in the regions that represent dorsal continuations of the interbuttress regions. The peculiar structure of the buttresses can be seen internally on the ridges that extend proximally. The origin of the centrodorsal is at the proximal apex. Thus, the stereomic microstructures have been consistent during the growth of the centrodorsal.

BASAL PLATE

In most Paleozoic crinoids, the basal or infrabasal plates were the points of attachment for the stem. Conditions in most Comatulida are quite different, although basals persist in Isocrinida such as *Endoxocrinus* and *Neocrinus*.

The lower (dorsal) inner surface of each basal in *Endoxocrinus* (Pl. 7,*1,2*) contains a deep depression where one-fifth of the proximalmost stem plate was attached as part of a symplexial suture. Its outline corresponds to a petaloid areola in the center and crenulae of one-fifth of the petalodium laterally. The pores of the stereom of the areola are nearly circular in outline and show some rectlinear arrangement. The pore area is 40 percent and pore diameter is 0.013-0.019 mm; pore area is slightly less than on stem plates but pore diameter is in the same range. The stereom of the areola is galleried as is that of the tops of the culmina. The pores of the stereom of the crenellae are larger (0.017-0.023 mm) and more irregular. The sides of the

culmina again have vertical ribs that act as supports. The larger pores seen in the petalodium of the stem also pierce the dorsal surface of the basal in an analogous position. The outer lateral and outer edges of each basal curve downward, so that the upper stem plate is partly recessed in a concavity. The symplexy with the basals is thus buffered against direct lateral shear. The stereom on the outer edge of the basal is dense with very small pores and a low pore area. The stereom of the upper (ventral) surface of the basals that is in contact with the radials is porous, but irregular in appearance.

The lumen of the stem is continuous into the interior of the calyx. The inner face of each basal forms one-fifth of the wall of the lumen. As the lumen is traced ventrally into the calyx, it bifurcates, producing a Y-shaped groove on the inner face of the basal (Pl. 7,*3,4*). The stereom within the center of the Y is galleried, indicating the presence of ligaments; pore diameter is 0.014-0.021 mm. The resultant funnel-shaped axial space at the internal juncture of the five basals is the position of the main aboral nervous center. The larger pores noted in the petalodium of the stem plates and basal facet open into the funnel-shaped space, supporting their interpretation as nerve canals. Other large pores appear to lead off horizontally into each basal from near the top of the Y.

The configuration of the articulum on the basals of *Neocrinus* is similar to that of *Endoxocrinus*. The configuration of the nerves that pass upward into the radials differs slightly, however. Instead of simply lying in a groove which opens out into a Y on the inner face of the basal, the nerves enter the basal halfway up its inner face (Pl. 7,*7,8*) and bifurcate to pass out through two holes 0.2 mm in diameter on the upper inner surface (Pl. 7,*5*), there to enter the lower surfaces of adjacent radials. Some infilling comprised of a very porous stereom occurs in these canals.

Basal plates are prominently developed in a Millericrinida such as *Democrinus,* but the tight adhesion of the plates does not permit ready disarticulation. Surface pore area is very low except where apparent solution or resorption has removed the external surface. This is seen externally as an irregular depressed equatorial ring (Pl. 7,*6*).

In contrast to other modern Comatulida, except for *Atopocrinus* (Breimer, in press), the genus *Atelecrinus* has well-developed basal plates in the mature organism. The basals separate the radials from the centrodorsal, the upper surface of which with its buttresses was described earlier. The lower surface of each basal is indented medially to fit over the buttress (Pl. 6,*3,4*). The stereom of the lower medial surface of the basal is not as strongly differentiated as in the corresponding buttress. A porous knob is present internally. The lateral lower surfaces of the basal that fit into the interbuttress depressions of the centrodorsal have denser stereom. Each basal has two flange-like processes that project internally, dividing the central space of calyx into a circle with five broad petaloid extensions (Pl. 6,*5,6*). Each petaloid area is centered on a basal and probably is the area where the nerve canals from the aboral nerve ring extend upward and bifurcate to extend into the central lumen of adjacent radials. This position would be analogous to the configuration of the nerve channels and canals on the inner faces of the basals of the Isocrinida *Endoxocrinus* and *Neocrinus* and the canal of the basal rays of the Comatulida *Comactinia.*

RADIAL PLATE

In the modern Articulata, the five radials form part of the cup and the arms are attached to them by a muscular articulation. The general form of the articulation is the same in the muscular articulation of primibrachials and succeeding brachials and will be discussed with them.

The radials of the isocrinid *Endoxocrinus* are similar in shape to those illustrated by Breimer (in press) for *Neocrinus.* The lower surface of the radial has a sharp median ridge with two concave, downward-sloping sides that fit against the ventral surface of two subjacent basals. The V-shaped bifurcation of the aboral nervous system on each basal, illustrated in Plate 7,*3,4,* continues upward in the radial as a pair of canals. These canals are 0.22 mm in diameter and pierce the dorsal inner surface of the radial 0.73 mm from the outer edge. They converge to a single opening on the muscular articulum. Another canal enters the radial on each of its inner sides. These canals are part of a pentagonal ring that

runs through the radials and they converge within each radial just behind the muscular articulum.

These canals are elliptical in cross section and larger in diameter (0.18 mm by 0.30 mm) than the canals on the lower surface. The pore area of the inner lateral surface of the radial near the lateral canal is 40 percent. Pores are ovoid with diameters of 0.010 to 0.023 mm; the stereom is irregular. The stereom lining the lateral nerve canal is smooth, whereas a few needlelike spikes of the stereom project into the dorsal nerve canal. The stereom of the dorsal surface of the radial also has a pore area of 40 percent with an irregular stereom; pore diameter is 0.009-0.018 mm. Both the lateral surfaces (radial-radial) and dorsal surfaces (radial-basal) are synostoses by definition. The pore diameter and pore area on the external surface of the plate are reduced.

Because of the adherence of the radial and basal plates in the Millericrinida *Democrinus,* it is necessary to fracture the calyx to reveal the internal nerve canals (Pl. 8,*3,4*). The aboral nervous center is located within a vertical cylinder formed by the basal and radial plates. The stereom of the walls of the cylinder formed by the basals has larger pores than that of the radials. The upper end of the cylinder subdivides into five canals that lead upward to the horizontal and vertical canals leading to the radial articula. On the exterior of the radial, the pore area is only about 10 percent and pore diameter is 0.002 mm.

Nerve canals similar to those of *Endoxocrinus* are found in the comatulid *Analcidometra.* The elliptical lateral canal (diameter 0.10 mm) enters the lateral face of the radial (Pl. 9,*1*) in a similar position, but the nerve cords from the aboral nerve center enter the inner face of the radial rather than the dorsal face (Pl. 8,*5,6*). The elliptical inner nerve canal is 0.11 mm in diameter. Both quickly merge inside the radial and are continuous with the lumen on the muscular articulum of the radial. The pore area of the lateral surface of the radial is 35 percent and pore diameter is 0.005 to 0.013 mm. The stereom is irregular and pores are ovoid. The stereom of the upper surface of the radial is less porous.

The configuration of the radial nerve canals in *Nemaster* (Pl. 9,*5,6*) is the same as that of *Analcidometra.* The maximum diameter of the elliptical lateral and inner canals is 0.43 mm. They merge a short distance internally; in one radial, they share a common opening. The lateral surface of the radial has some low ridges with denser stereom along its ventral margin as well as some within the lateral edge (Pl. 9,*2-4*). The stereom is galleried between the ridges along the ventral margin. Pore area is about 50 percent; pore diameter is 0.009 to 0.016 mm. The functional significance of these ridges on a synostosial suture is not understood. A groove along the bottom of the lateral face marks an indentation by a basal ray. The stereom within the groove is irregular with ovoid pores. The pore area is 50 percent and pore diameter is variable, from 0.012 to 0.040 mm. The pore area of the stereom bordering the groove is 30 percent and pore diameter is smaller, 0.010 to 0.023 mm. The stereom is irregular.

In *Comactinia,* as in *Nemaster,* the basal rays occupy interradial positions beneath the lateral edges of the radial, separating these edges from the centrodorsal. The inner edge of the basal rays form a convergent hood over the cavity within the centrodorsal (Pl. 8,*1,2*). The nerves that enter the inner face of the radials first pass through two canals in the basal rays.

The radials of *Atelecrinus* show a different arrangement of the nerves. The lumen of the muscular articulum is a large ovoid opening (greatest diameter 0.041 mm). The lumen does not bifurcate but opens into a void on the internal face of the radial. The two flanges on each basal described earlier (Pl. 6,*5,6*) curve upward to connect with similar flanges coming down from the center of each overlying radial (one per radial). The effect is to produce a donut-shaped space with ten bands around it (the flanges), which corresponds to the lateral nerve canal of other radials. The lumen of the muscular articulum opens internally into this space. The petaloid areas centered on each basal between the flanges represent a space for the upward passage of the inner (or dorsal) nerve cords to the radial.

ARTICULATIONS

The brachial plates of the arms of Recent crinoids articulate with one another along several kinds of sutures: a muscular articulation, a

syzygy, a symmorphy, or a synarthy. The stereom reaches its greatest differentiation in microstructure in muscular articulations and the types of tissue present are reflected in the patterns of the stereom. The collagenous nature of some of the ligaments has been examined by Meyer (1971).

MUSCULAR ARTICULATIONS

The basic structure of a muscular articulation is a lower (dorsal) ligament fossa for the extensor ligament, a transverse bar, the fulcral ridge, which may be horizontal or oblique, a subcentral lumen for the brachial nerve, which is above (ventral) the fulcral ridge, two fossae lateral to the lumen for the interarticular ligaments, and two fossae above these for flexor muscles (*see* Pl. 11,*2*). The interarticular ligaments and flexor muscles cause an arm to enroll. The muscle fossae commonly appear as two ears. The space in between is occupied by part of the aboral coelomic canal. The ambulacral groove is still some distance above this and not directly reflected in the brachials (see Breimer, in press).

Endoxocrinus of the Articulata lives in depths of 100 to 600 m. These regions usually have currents that cause the arms to form a filtration fan in which the fan is tilted, the food groove is downcurrent, and the arms partially recurve back into the current. The muscular articulation of the arms (Pl. 10,*1,2*; 11,*2*) shows a prominent fulcral ridge as on the radial; the fulcral ridge has a small amount of abrasion. Its stereom is almost solid (Pl. 11,*3,4*). The fulcral ridge and the stereom around the lumen of the radial are the highest areas on the articulum. The dorsal ligament fossa is broad and concave and is deepest medially by the fulcral ridge. The two ventral ligament fossae are also concave. Each upper edge turns upward to a ridged border with the muscle fossa. Each of the latter are also slightly concave. The lumen is a large elliptical opening 0.3 by 0.6 mm; it bifurcates internally. A deep cleft, the intermuscular furrow (e.g., Pl. 10,*3,4*), separates the muscle fossae, but does not reach the lumen. It represents a dorsal extension of the aboral coelomic canal. The stereom of the floor of the intermuscular furrow has large pores, 0.024 to 0.040 mm; pore area is about 30 percent. The dorsal fossa is broad and deep; the stereom is well galleried, indicating the presence of long ligament fibers (Pl. 11,*1*). Pore area is 45 percent and the ovoid pores are 0.008 to 0.021 mm in diameter.

The ventral ligament fossae are also well galleried and pore area is 35 percent. The ovoid pores are slightly larger on the average, with diameters ranging from 0.013 to 0.025 mm. The structure of the stereom in a muscle fossa is quite different. Superficially, the fossa looks like the floor of a cave with innumerable stalagmites pointing into the fossa (Pl. 11,*5,6*). Beneath this is a more open irregular porous stereom with a pore area of 45 percent and pore diameters of 0.009 to 0.020 mm. The formation of the stalagmites represents a change in the growth pattern in the muscular fossa. The diameter of the bars and rods decreases from 0.006 to 0.007 mm to 0.002-0.003 mm. The stalagmites grow upward, but in continuity with the older stereom. There are some cross connectives that also form; pore diameters are smaller (ranging from 0.007 to 0.016 mm) and pore area is reduced to 15 to 30 percent. Some parts of the fossa show greater acceleration in the production of stalagmites, producing a clotted appearance in the fossa. In the ligament fossae, the ligament fibers penetrate into the stereom. In contrast, muscle tissue does not penetrate into the stereom, but is in contact only on the surface. The effect of the formation of stalagmites is to produce a greater surface area with greater surface relief. Presumably this is related to the attachment of the muscle to the stereom of a muscle fossa.

The patterns found on the muscular articulum of the radial are also found on the opposing face on the IBr_1. The suture between IBr_1 and IBr_2, an axillary, is a synarthry (see "Synarthry"), but the distal face of the IBr_2 again has two muscular articulations with the same stereomic patterns. The change in the pattern of the stereom from the ventral ligament fossa to the muscle fossa is again abrupt. The central lumen of each facet has decreased in size slightly, to 0.33 by 0.45 mm.

Muscular articulations are very common in the more distal brachials. The relative area of the articulum above the fulcral ridge has increased, but stereomic microstructure remains the same. The muscular fossa is smoother in its appearance, the clotted effect being absent. Stalagmites are not as prominent, are more evenly developed, and do not have as great a vertical expression.

There is a small knoblike buildup in the dorsal corners of the fossae adjacent to the intermuscular furrow. The surface of the plate drops from the ventral ligament fossa into the muscle fossa (Pl. 10,*5,6*). Pore diameter in the ventral fossa remains almost the same (0.010 to 0.024 mm) as in the radial articulum (0.013 to 0.025 mm). The diameter of the central lumen continues to decrease (0.21 mm); its interior is almost smooth, being lined with irregular stereom.

Neocrinus lives in environments similar to *Endoxocrinus*. The proximal articulum of IBr_1 of *Neocrinus* is a muscular articulum; it faces the radial. The dorsal ligament fossa is again large and galleried; the pores are somewhat polygonal. Pore diameter is 0.005 to 0.012 mm; pore area is 40 percent. Pores of the ventral ligament fossae are ovoid and galleried; pore diameter is larger (0.009 to 0.017 mm) and pore area about 50 percent. Stalagmites are again developed in the muscle fossae (Pl. 12,*1-4*), covering a more open irregular stereom (e.g., Pl. 12,*5,6*); the fossae have a clotted appearance due to greater development in one area than another. The intermuscular furrow is prominent, but does not extend to the lumen. Basic stereomic patterns in the muscular articulations of the Isocrinida thus appear to be similar.

Democrinus, a millericrinid, inhabits waters of several hundred or thousands of meters in depth. Currents are prevalent in the regions where it occurs. The five arms are fanned back against the current to form a filtration fan. The muscular articulations of the arms partially differ from those of an isocrinid. In *Democrinus,* the muscular articulation between the radial and Br_1 is large and prominent (Pl. 13,*1*). The area of the dorsal ligament fossa, however, is smaller compared to the fossae above the fulcral ridge (Pl. 13,*3,4*). The latter are deeply concave. The stereom of the dorsal ligament fossa of the radial does not have an open galleried structure. There is an ovoid area in the central part of the fossa and in the ligament pit where the bars of the stereom on the surface have been widened by blocky overgrowths, thus reducing the pore area of the stereom (it is about 30 percent). Pore diameter is 0.003 to 0.013 mm. The transverse bar is almost solid; the diameter of the lumen is 0.08 mm. The stereom of the ventral ligament fossae shows typical gallery structure and has a higher pore area; pore diameter is 0.007 to 0.013 mm. The transition from the ventral ligament fossa to the muscle fossa is abrupt, being nearly vertical (Pl. 13,*5,6*); the stereom of the transition region has some blocky overgrowths. The stereom within the concave muscular fossa is an open irregular mesh; pore diameter is 0.007 to 0.020 mm. The stereom on the upper lateral edges of the muscle fossae shows prominent blocky overgrowths (Pl. 13,*2*). The proximal face of the Br_1, which is in opposition to the radial, has a more typical appearing muscular articulum (Pl. 14,*1,2*). Blocky overgrowths on the stereom are lacking. The dorsal ligament fossa has typical gallery structure as does the ventral ligament fossa. Pores are ovoid in both and diameters are 0.007 to 0.011 mm and 0.007 to 0.014 mm, respectively. The muscle fossa lies topographically below the level of the ventral ligament fossa and its stereom is irregular (Pl. 14,*3,4*); the ovoid pores interconnect, but there is no continuous line of them internally. This type of structure is typical of the muscle fossae of most Comatulida and is referred to as labyrinthic structure. Its pore area is 40 percent in *Democrinus* and the pore diameter is 0.007 to 0.016 mm. The intermuscular furrow forms a groove that extends to the lumen on muscular articula beyond Br_1.

Nemaster rubiginosa is a shallow-water genus of Comatulida which avoids currents, living with the calyx concealed at one site for a long period of time, arms extended multidirectionally into the surrounding water mass. In the muscular articula of the brachials (Pl. 15,*3,4*), the dorsal ligament fossa is large and well developed, its surface area comprising about half that of the articulum. The ventral ligament fossae are also well developed; the muscular fossae are rather small by comparison. The stereom of the dorsal ligament fossa is galleried throughout. The pores are ovoid to polygonal within the ligament pit, becoming ovoid and slightly smaller toward the dorsal periphery of the fossa. There are also concentric bands, representing growth increments. Pore area exceeds 50 percent in the ligament pit and is about 50 percent outside it; pore diameter is 0.005 to 0.009 mm in the pit, 0.003 to 0.010 mm outside it. Dense, nonporous spines border the dorsal fossa on a distal muscular articulum. The ventral fossae are also galleried; the pores are ovoid with diameters of 0.004 to

0.008 mm; the pore area slightly exceeds 40 percent. The stereom of the muscle fossae lies below the level of the ventral fossa and is labyrinthic with ovoid pores (Pl. 15,*5,6*). There are small pointed projections from the stereom. Pore area is nearly 25 percent and pore diameters range from 0.003 to 0.006 mm. The stereom is coarser and pores have a larger average diameter than the ventral ligament fossa. An intermuscular furrow with very coarse stereom extends toward, but does not reach, the lumen. The diameter of the lumen is 0.38 mm on IBr_2, but decreases distally. The fulcral ridge is somewhat porous and shows signs of abrasion, due to rotation against the opposing face (Pl. 16,*1,2*).

There are some differences in the stereom of the muscular articulations of IBr_2 (axillary). The muscle fossae are separated from the ventral ligament fossa by a ridge; they extend farther laterally than vertically. The intermuscular furrow extends to the lumen.

In contrast to *Nemaster rubiginosa, Analcidometra* is a current-seeking form, which is usually found attached to alcyonarians. It usually extends its arms in one plane to form a filtration fan, and if stimulated, can swim, moving the ten arms in four different groups; each arm moves four times in five seconds. The dorsal ligament fossa (Pl. 16,*3,4*) occupies one-third or slightly less of the total area of the articulum and is deeply concave. The fulcral ridge and the area around the lumen (whose diameter is 0.1 mm) are the highest points on the articulum. The ventral ligament fossae are well developed. The muscle fossae are larger and set at a lower level (Pl. 16,*5,6*). A porous intermuscular furrow (developed here as a bridge) leads toward the lumen. The fulcral ridge shows traces of abrasion. The ligament fossae are galleried; the pores are coarsest in the dorsal ligament pit. The muscular fossae have a labyrinthic stereom with pores larger (0.004 to 0.014 mm; 40 percent pore area) than those of the adjacent ventral ligament fossae (0.003 to 0.007 mm; 50 percent pore area).

Ctenantedon is a current-avoiding genus of Comatulida found within the infrastructure of a reef at depths of 10-40 m. It is almost never exposed at day or night. If agitated, it is capable of very rapid simultaneous flexure of the arms to produce a crawling-swimming motion. The structure of its muscular fossae is quite different than that of other Articulata. The dorsal ligament fossa occupies about one-third of the surface area of the muscular articulum (Pl. 17,*3,4*). It is concave, being deepest in the ligament pit adjacent to the fulcral ridge. The stereom is galleried; pores are subpolygonal to ovoid. Pore diameter is small (0.001 to 0.005 mm) and pore area is 50 percent. The structure and pore area of the stereom of the ventral ligament fossae is the same; pore diameter is 0.002 to 0.006 mm. The surface of the articulum rises from a ventral ligament fossa into the muscular fossa instead of dropping (Pl. 17,*5,6*). The stereom of the muscle fossa has distinctive concentric bands and is almost a solid sheet with short vertical spikes projecting off it. Pore area is only about 15 percent; pore diameter is 0.003 to 0.006 mm. A muscle fossa with this density or structure has been found only in *Ctenantedon* to date. It might be related to stresses generated by the rapid contraction of the arms. A broad, porous, intermuscular furrow is present; it is elevated slightly above the dorsal apex of the muscular fossae. The elliptical flat-floored lumen is 0.12 mm in diameter.

Crinometra is a genus of Comatulida found from 150 to over 500 m. Its living habits have not been directly observed, in contrast to those of the genus discussed above. Its muscular articulations (Pl. 18,*1*) appear very similar in their microstructure to those of other Comatulida such as *Comactinia* and *Nemaster*. One difference, however, is the presence of an elevated knob that has developed in the dorsal apex of each muscle fossa (Pl. 18,*2*); a similar feature is found in *Endoxocrinus*. The pores of the knob have about the same dimensions as those of the ventral ligament fossa, but the bars of the stereom are thicker. Its functional significance is unknown. The intermuscular furrow is a groove that extends almost to the lumen.

Atelecrinus is a deeper-water genus of Comatulida found from 500 to 1500 m. Its life habits have not been directly observed. It is noteworthy for the extreme development of its muscular fossae (Pl. 18,*3,4*), the concavity of all its fossae, and the differences in its stereom. The dorsal ligament fossa is not large and the galleried stereom occupied by ligaments are more medially restricted than usual. Galleries are somewhat superficial. Pores have a polygonal outline

and diameters of 0.003 to 0.008 mm; pore area is 40 percent. The fulcral ridge shows signs of abrasion on its lateral edge; the lumen is large (0.3 mm). Calcification along its dorsal floor is not always complete and there is sometimes an opening from the ligament pit. The stereom of the ventral ligament fossa is not galleried, but is labyrinthic (Pl. 19,*1*). The upper pores are small (0.002 to 0.006 mm) in contrast to those of the coarser muscular fossa (0.008 to 0.017 mm) (Pl. 18,*5,6*). Pore area in both fossae is 40 percent. The muscle fossa shows concentric growth bands. An intermuscular furrow is lacking. In two IBr_2 (axillary), there is a peculiar, massive, oval structure developed on the ventral lateral margin of the muscular fossa (Pl. 17,*7,8*; 18,*3,4*). It faces laterally and has a horizontally grooved surface. The ridges are sharp and composed of denser stereom that has built upward from the surface. If the two oval structures interlocked with one another, they would have provided a rigid support at the base of the arms.

SYZYGY

A syzygy is a ligamentary articulation in which the culmina (ridges) of one articulum are opposed to the corresponding elevations of the other articulum. The culmina radiate from the lumen. The ligaments are located primarily in the crenellae between the culmina and therefore appear as a series of dots along the suture where syzygy is present. The syzygy allows limited mobility in all directions. It is typically developed only in the Comatulida.

The syzygial articulum of the comatulid *Nemaster* (Pl. 19,*2*) has a slightly raised rim around the ventral part of the lumen and several culmina, which radiate from a place at or near the lumen (Pl. 19,*6*) out to the periphery of the plate (Pl. 19,*3,4*). As the distance between these radiating culmina widen, newer ones are inserted to fill partially the widening space. The primary culmina are nearly, but not quite straight. The top of each culmen is composed of knobby, massive stereom with some small pores (diameter 0.002 to 0.005 mm) between the knobs (Pl. 19,*5*). Abrasion marks are visible on the tops and sides of some of the knobs. The stereom of the intervening crenellae is porous (50 percent); pore diameters vary from 0.002 to 0.005 mm. There is some internal regularity in pore form.

The syzygial articulum of *Comactinia* is very similar to that of *Nemaster*. An elevated area again surrounds the ventral side of the lumen. The culmina are not quite as knobby. Their pore area is ten percent; pore diameters are 0.002 to 0.008 mm. The stereom of the crenellae is very porous and has a well-developed gallery structure. Pore diameters vary from 0.001 to 0.005 mm. Pore area is 50 percent.

The culmina of a syzygy of *Ctenantedon* (Pl. 20,*1,2*) are broad and flat and stand fairly high above the surface of the plate. The stereom of the intervening crenellae is very porous, but not galleried.

The culmina of a syzygy in *Analcidometra* (Pl. 20,*3,4*) are not radially arranged as those described above. There is a raised area around the lumen. The culmina are raised areas, peripherally located. Their form is either a knob or an arcuate, convex, inward extension. The stereom is thickened into knobs to produce them. There are larger pores in the crenellae around the lower half of the lumen and two areas ventral to it on either side. The stereom of these areas is galleried, whereas in the other parts of the crenellae of the articulum, it is not.

In *Atelecrinus* the culmina are fainter (Pl. 20,*5,6*). The central area around the lumen is commonly broadly exposed and the outline is irregular and ragged. Knobs are present along the culmina, but the stereom is more porous. The stereom of the crenellae is porous, but is not galleried.

SYNARTHRY

A synarthry is a ligamentary articulation in which the opposed articula each bear medial fulcral ridges which are aligned with one another. Each articulum has relatively broad bifascial ligament fields next to the fulcral ridge, which permit mobility in a direction normal to the axis of the fulcral ridge. Synarthries may also be present in the stem and cirri (e.g., Pl. 2,*4*).

In the brachials of the comatulid *Comactinia* (Pl. 21,*1,2*), the fulcral ridge of the synarthry forms the highest area on the articulum. The fulcral ridge has small pores and is moderately porous. It has developed a medial groove ventrally and has considerable evidence of abrasion. The stereom of each of the bifascial ligament fields is galleried. Pores are larger near the lu-

men (0.005 to 0.009 mm; pore area 35 percent); these decrease in diameter to .001 to .006 mm peripherally and porosity increases to 50 percent. Inner pores are ovoid; outer pores are ovoid to subpolygonal.

In *Analcidometra* the dorsal half of the fulcral ridge is more strongly differentiated than that of the ventral half (Pl. 21,*3*). The stereom of a bifascial ligament field is not galleried and has a pore area of 50 percent. The pores are ovoid with diameters of 0.003 to 0.008 mm.

A synarthry in *Atelecrinus* has a broad fulcral ridge (Pl. 21,*5,6*). Dorsally, it is flat on the upper surface with horizontal lines of pores; pore area is low. Ventrally the ridge is more rounded and massive. The stereom around the lumen is coarse and elevated. The bifascial ligament fields are deeply concave; there is some concentric banding in their stereom. The pores are subpolygonal and 0.002 to 0.008 mm in diameter. The stereom is not galleried.

There is another type of synarthry, a trifascial articulation, which occurs in the Millericrinida. Instead of two ligament bundles there are three. Its configuration can be seen in the brachials of *Democrinus* (Pl. 14,*6*; 15,*1,2*). The ventral fulcral ridge remains unaltered, but the dorsal ridge has been replaced by two ridges, which radiate dorsally from the central lumen at a low angle. The fulcral ridges widen away from the lumen. The stereom is thickened to form knobs. The stereom of the trifascial ligament fields has well-developed gallery structures. The ovoid pores are 0.004 to 0.008 mm in diameter; pore area is 40 percent. In more distal brachials, the fulcral ridges are comparatively more massive.

A trifascial synarthry occurs between IBr_1 and IBr_2 in the Isocrinida *Neocrinus*. The hypozygal *(IBr_1)* articulum is illustrated in Plate 21,*4*. It is basically convex. The stereom ventral to the lumen is not strengthened except for a small area immediately ventral to the lumen. Two fulcral ridges extend dorsally from the lumen to the dorsal margin. Their stereom is dense and nonporous. They define a small triangular medial field with galleried stereom; there are two large lateral fields as well, some parts of which are galleried. The stereom of the ventral center of the epizygal face is denser. The region immediately dorsal to the lumen has a groove; the two fulcral ridges lie dorsal to this. The lateral ligament fields are concave. This articulation permits limited lateral movement of an arm at its base.

SYMMORPHY

By definition, a symmorphy is a ligamentary articulation in which a prominent transverse culmination of the epizygal (Pl. 22,*3,4*) brachial fits into a corresponding depression of the hypozygal (Pl. 22,*1,2*). It is not a common type of articulation, but is found in the brachials of *Neocrinus*. The central flatter portion of the articulum has numerous galleried pores (pore area 50 percent; pore diameter 0.004 to 0.013 mm). Sharp dense culmina border this area. In the dorsal part of the articulum they are radially arranged (Pl. 22,*5*). Laterally they run parallel to the border of the articulum and may be relatively long. The hypozygal has two deep lateral depressions, whereas the epizygal has two sharp lateral prominences.

Some ligamentary articulations in the arms do not clearly fit any of the types described above. Such is the articulation between IBr_1 and IBr_2 (axillary) in the Isocrinida *Endoxocrinus* (Pl. 22,*6*; 23,*1*). There is a heart-shaped fossa in the middle of the plate, centered on the lumen. It is concave on both articula. The intermuscular furrow extends down to it. The stereom of the fossa is irregular, with ovoid pores smaller (0.007 to 0.016 mm) than that outside (0.010 to 0.019 mm), and pore area is near 35 percent inside, 45 percent outside. There are a few low dorsal ridges in the fossa on IBr_2, but they are lacking in IBr_1. Some low culmina occur along the dorsal lateral edges of each articulum outside the fossae. These are short and irregular in their expression. Knobs are developed in the stereom on top of the culmina in some places. The stereom in between shows a few galleries, but is mostly irregular. The same type of articulation exists between an axillary brachial and its proximal brachial. The fossae have disappeared to be replaced by a flat surface. Such an articulation probably represents an example of a cryptosymplexy (Breimer, in press).

BRACHIALS

The ovoid or angular brachial plates serve as skeletal supports for the tissues of the arms and as points of articulation for the pinnulars. Some

are massive, others very delicate. In the isocrinid *Endoxocrinus,* the external stereom of the brachial (Pl. 23,*2*) has a pore area of nearly 25 percent and pores with diameters of 0.011 to 0.025 mm. The exterior surface of the brachials of the Millericrinida *Democrinus* are relatively porous. The broad proximal brachials have developed peculiar knobby processes on the ventral surface (Pl. 14,*5*). The exterior surface of the primibrachial of the comatulid *Nemaster* (Pl. 23,*3*) has pores that have some arrangement in rows. Pores are ovoid with diameters of 0.006 to 0.022 mm, pore area is nearly 15 percent. Similar linear patterns can be seen on more distal brachials. The exterior surface of a brachial in *Comactinia* (Pl. 23,*4*) is relatively porous; the pores show diagonal arrangement. The stereom of *Analcidometra* (Pl. 17,*1,2*) is very porous and open, whereas in contrast, that of *Ctenantedon* is dense and has some linear arrangement of the pores.

PINNULES

The plates of the pinnules display a wide variety of form and structure in different genera. In the isocrinid *Endoxocrinus,* the pinnulars are trough-shaped (Pl. 24,*5,6*). The ventral trough may show three or four scalloped areas along its walls. The tops of these mark the site of attachment of ambulacral cover plates. A canal (diameter 0.065 mm) pierces the axis of the plate. The stereom of the plate is an irregular open mesh on the surface of the plate. The mesh along the floor of the trough is not always complete and the axial canal can be seen from a ventral position. The stereom lining the axial canal has long straight ribs with regularly spaced pores (Pl. 25,*1*). The pores are alternately offset on either side of a rib. The articulation between the first and second pinnulars has the same form as a muscular articulation of the brachials; the microstructure of the stereom is also the same. In more distal pinnular articulations, the form of this articulation becomes slightly modified (Pl. 25,*2-4*). A long horizontal or oblique fulcral ridge is absent. Instead, there is an area just dorsal to the lumen where there is thickened stereom; two ridges with thickened stereom (the expression is variable) extend diagonally downward in a dorsal direction. These areas serve as a fulcral surface. A triangular dorsal area contains a ligament pit; the stereom is galleried. Two areas lateral to the lumen also have galleried stereom. Ventral to these are two small concave areas with irregular stereom (labyrinthic). This is a muscular articulation, with ligaments dorsally and laterally, and muscles ventrally. Pore diameter in the lateral area ranges from 0.010 to 0.023 mm. In the most distal pinnules, the muscle fossae appear to be absent.

The articulation between the proximal pinnule and the brachial is also a muscular articulation, but its form is modified ventrally. The pinnular articulum is located on the upper lateral surface of the brachial (Pl. 10,*1,2*; 23,*5,6*). The surface rises proximal to the articulum, forming a wall. The fulcral ridge extends the full width of the articulum and is at an angle of 50° to the axis of the brachial (Pl. 24,*1,2*). It is also at a high angle to the fulcral ridge of the next pinnular articulation. The stereom of the area in the lower (proximal) part of the articulum is galleried and there is a prominent ligament pit. Pores are ovoid to subpolygonal with diameters from 0.006 to 0.028 mm. The lumen of an axial canal (diameter 0.10 mm) is present just above (distal) the fulcral ridge. The stereom on either side and immediately above the lumen is galleried; pore diameters are 0.006 to 0.030 mm. It is more extensive toward the outer edge of the brachial. Distal to the lumen, there is a large, deep concavity forming the entire upper part of the articulum. The two ear-shaped fossae characteristic of muscular articulations are absent. The muscles are concentrated in one area, extending into this deep concavity (the muscle concavity) whose sides are smooth and which ends blindly. The coarse stereom along the axis of the brachial that lies beneath the aboral coelomic space is adjacent to the inner edge of the muscle concavity. The stereom of the muscle fossa on the proximal surface of the first pinnular is labyrinthic (Pl. 24,*3,4*).

The pinnular facet is located on the upper distal surface of the brachial of *Neocrinus* (Pl. 12,*1,2*). The fulcral ridge is slightly porous. There is a well-developed dorsal (proximal) ligament fossa with a deep ligament pit and galleried stereom (Pl. 25,*5,6*). The stereom of the ventral (distal) ligament on either side of the

lumen (diameter 0.075 mm) is also galleried. The muscle concavity in the upper center of the articulum is exceptionally large and deep.

The pinnulars of the millericrinid *Democrinus* are also trough-shaped (Pl. 27,*1,2*). A canal penetrates the center of the plate. The articulation between the first and second pinnulars is a muscular articulation (Pl. 26,*5,6*). A well-developed ligament pit occurs below the transverse fulcral ridge. This is the primary area of flexure in the pinnule. Subsequent pinnular articulations are characterized by an absence of muscular fossae, but have galleried stereom on the articular surfaces (Pl. 27,*3,4*). The configuration of the articulation between the proximal pinnular (Pl. 26,*3,4*) and the brachial (Pl. 26,*1,2*) is very similar to that of *Endoxocrinus*. A ligament pit, transverse fulcral ridge, lumen, and muscle concavity are well developed.

In the comatulid *Nemaster,* the shape of the pinnular is different. In *Democrinus* and *Endoxocrinus,* the tube feet can withdraw into the U-shaped trough. In *Nemaster,* the pinnular has become rod-shaped and functions as a supporting shaft in the tissue (Pl. 28,*4*). The ambulacral system lies above the ventral surface of the plate and there is no space in the upper surface into which the tube feet may contract. The upper (ventral) surface of each pinnular has a shallow broad groove running lengthwise. On the proximal pinnulars, several small lumens open downward into the plate from this groove. In more distal pinnulars, there are two small lumina located in the distal part of the groove; others may be present proximally (Pl. 28,*5*). These all die out internally, and do not appear to connect directly with the axial canal.

The brachial-pinnular articulation in *Nemaster* is on the upper lateral surface of the brachial (Pl. 15,*3,4*). The articulum on the brachial (Pl. 27,*5,6*) is ovoid and its general plan resembles that of *Democrinus* and *Endoxocrinus*. There is a transverse fulcral ridge and a well-developed dorsal ligament fossa with ligament pit and galleried stereom. A large lumen lies immediately above the fulcral ridge and lateral to this are two areas occupied by ligaments. The upper center of the articulum has three or four concavities that appear to correspond with the muscular concavity of the brachial-pinnular facet of *Democrinus* and *Endoxocrinus*. The opposing articulum of the first pinnular (Pl. 28,*1,2*) has galleried stereom in the ligament fossae. The muscular fossa, a single, slightly concave area in the upper center, has labyrinthic stereom. The first three pinnulars are short. The articulation between the first and second pinnulars is a muscular articulation in which the shape of the articula is like that found between the brachials. This shape is modified distally, however, so that all the longer pinnulars have the configuration seen in Plate 28,*6,7*.

On the proximal surface of a pinnule, three massive ridges radiate from the lumen; they may or may not reach the periphery of the articulum (Pl. 28,*3*). They have few pores. One ridge goes up (ventrally); two radiate laterally downward. On the distal surface, the upper ridge is replaced by a groove (Pl. 28,*6,7*), which probably limits slippage between the two plates. Two arcuate areas in each upper lateral corner are the muscle fossae. They are depressed below the surface of the rest of the articulum and have a different stereomic microstructure. Otherwise, areas between and beyond the ridges are galleried, indicating the presence of ligaments. The distal margin of each pinnular bears distally projecting nonporous spines; these occur on the lateral and dorsal borders. The terminal pinnular has spines that are recurved proximally, providing grapnel-like hooks. The proximal articulum of a pinnular has beveled edges (Pl. 28,*4*), whereas that on the distal end has a flatter aspect except for the projecting spines. The succession of proximal beveled edges allows for a great deal of flexure between successive pinnulars and allows the pinnules to effect a writhing and lashing motion.

The pinnular-brachial articulation of *Comactinia* is located on the upper lateral surface of the brachials. The articulum on the brachial is ovoid (Pl. 29,*1,2*). The fulcral ridge is straight in the proximal half of the articulum, but bent toward the lower part of the articulum distally. There is a prominent ligament pit in the lower part of the articulum, surrounded by galleried stereom. There is also galleried stereom on either side of the lumen, but it is more extensively developed distally. A deep muscle concavity appears in the upper center of the articulum. It is coextensive with an area with irregular stereom

in the upper distal part of the articulum. A less extensive shallow concavity occurs in the upper proximal part of the articulum. These apparently correspond to the two ears of a brachial muscular articulation; the proximal has been suppressed because of a lack of space. The pinnulars of *Comactinia* show many of the same features as *Nemaster,* such as modification of the muscular articulum to form a triradiate fulcral area (Pl. 29,*3,4*), shallow groove on the ventral surface (Pl. 30,*1,3*) with numerous holes or spines (Pl. 29,*5,6*), and others. Fulcral ridges may show evident signs of abrasion.

The brachial-pinnular articulation in *Analcidometra* is located on the upper distal surface of the brachial (Pl. 17,*1,2*; 30,*2*). The fulcral ridge is straight and contains some pores. It is formed by knobby thickenings of the stereom, which show signs of abrasion (Pl. 30,*4*). The stereom of the dorsal (proximal) ligament fossa is more open than that of other corresponding articula; a ligament pit is present. The lumen separates two ventral (distal) ligament fossae, of which the outer is more highly developed. The stereom is galleried, in contrast to the dorsal ligament fossa. The muscle fossa is a large triangular area that has coarse stereom with a wide range in pore diameters (0.006 to 0.036 mm). The muscle fossa is more highly developed next to the inner edge of the articulum; a muscular concavity is present along the lower inner edge. The corresponding articulum on the proximal surface of the first pinnular (Pl. 30,*5,6*) shows two differences: the stereom of the dorsal ligament pit is galleried and the part of the muscle fossa opposite the muscle concavity has massive stereom with some concentric bands.

CONCLUSIONS

The microstructure of the crinoid endoskeleton is highly reflective of the function of the plates. The symplexial articulations of the Isocrinida stems are strongly differentiated and the galleried pores for the long ligament fibers are larger in diameter than on other articular surfaces. Diameters are narrower on synostosial surfaces where breakage is easier. The synarthrial articulations of the Millericrinida have developed specialized knobs adjacent to the massive fulcral ridge to prevent lateral slippage. Both these and the bifascial ligament fields are produced by ontogenetic modification of a synostosial articulation. Pore area of the ligament fields in the stems is 40 to 50 percent.

The dorsal part of the ligamentary articulation of the cirri of modern crinoids has been enhanced to maximize the clasping function of the cirri. Diameters of the galleried ligamentary pores are smaller (0.002-0.007 mm) in the Comatulida than in the Isocrinida (0.009-0.018 mm). Pore area in both is usually nearly 50 percent, whereas the pore area of the stereom of the exterior of the cirri is reduced to nearly its lowest level with respect to any plate.

The interiors of crinoid plates are occupied by canals, which are extensions from the main aboral nervous center. These range in diameter from 0.038 mm in the very narrow accessory nerve canals of the stems of the Isocrinida to large canals over 0.4 mm in diameter in the radials of the Comatulida. Their geometrical configuration is complex. The main aboral nerve center is clearly reflected in the structure of the basals or centrodorsal.

The crinoid endoskeleton reaches its strongest degree of differentiation in the muscular articulations of the arms. Dorsal ligament fossae are galleried with a pore area usually between 40 to 50 percent. The pore diameters reach a slightly greater maximum in the stemmed crinoids, the Isocrinida and Millericrinida, than in the Comatulida. The fulcral bars are massive structures that may show abrasive wear. The ventral interarticular ligament fossae are usually similar to the dorsal fossa in their structure, pore diameter, and pore area. The muscle fossae, separated by an intermuscular furrow, have a variety of stereomic microstructures (usually labyrinthic), which reflect the attachment of the muscle to the surface of the plate and its nonpenetration, in contrast to the long ligament fibers, which penetrate into the plate in the galleries. The pore area of the muscle fossae varies from 15 to 40 percent dependent upon the type of microstructure; pore diameters are similar to those of the ligament fossae but more variable.

Other specialized ligamentary articulations of the arms such as synarthries, symmorphies, and syzygies usually also have galleried stereom for long ligament fibers. The pore area is 40 to 50 percent; pore diameters range from 0.001 to

0.013 mm. They have their smallest maxima in the syzygies (0.005 mm) and their largest in a symmorphy. Culmina and fulcral ridges have a variety of microstructures, from knobby to massive.

The geometric complexity of a crinoid plate reaches its highest level in the brachials and pinnulars. The surfaces may be extremely three-dimensional because of the lobes of the muscle fossae. The articulum of the pinnule on a brachial is a muscular articulation, with the geometry of the muscle fossae altered to form a single muscle concavity. The geometry of the muscular articulations between the first two or three pinnulars is similar to that of the brachials, but in following ones is modified to allow greater flexibility. The fulcral surface is no longer a straight bar, but usually has a triradiate pattern. The beveling of the lateral edges of the proximal ends of the pinnulars promotes even greater flexibility. In the stemmed Isocrinida and Millericrinida, pinnulars are trough-shaped, but in many of the Comatulida they are rod-shaped with shallow grooves on the upper surface with peculiar pores.

Stereomic microstructure is well enough preserved in some fossil crinoids to allow an interpretation of the evolutionary history based upon skeletal microstructure as demonstrated by Roux (1970, 1971) for Mesozoic-Cenozoic stem plates, and by Lane and Macurda (in press) for Paleozoic inadunates. The discovery of other suitably preserved material should provide further interpretative insight into the functional morphology and evolutionary history of crinoids.

REFERENCES

Breimer, Albert, in press, Recent crinoids: in R. C. Moore and Curt Teichert, eds., Treatise on Invertebrate Paleontology, Part T, Echinodermata 1 (Crinoidea).

Lane, N. G., & Macurda, D. B., Jr., in press, New evidence for muscular articulations in Paleozoic crinoids: Manuscript submitted to Paleobiology.

Macurda, D. B., Jr., & Meyer, D. L., 1974, The feeding posture of modern stalked crinoids (Echinodermata): Nature, v. 247, p. 394-396, fig. 1.

Meyer, D. L., 1971, The collagenous nature of problematical ligaments in crinoids (Echinodermata): Marine Biology, v. 9, p. 235-241.

Moore, R. C., Jeffords, R. M., & Miller, T. H., 1968, Morphological features of crinoid columns: Univ. Kansas Paleont. Contrib., Echinodermata, Art. 8, 30 p., 5 fig., 4 pl.

Roux, Michel, 1970, Introduction à l'étude des microstructures des tiges des crinoïdes: Geobios, v. 3, p. 79-98, pl. 14-16.

———, 1971, Recherches sur la microstructure des pédoncules de crinoïdes post Paléozoïques: Univ. Paris, Lab. Paléontologie, Trav., 83 p., 34 fig., 4 pl.

———, 1974, Les principaux modes d'articulation des ossicules du squelette des Crinoïdes pédonculés actuels. Observations microstructurales et conséquences pour l'interprétation des fossiles: Acad Sci. Paris, Comptes Rendus, v. 278, sér. D, p. 2015-2018, fig. 1-4.

Sprinkle, James, 1973, Morphology and evolution of fossil blastozoan echinoderms: Harvard Univ., Museum of Comp. Zoology, Spec. Pub., 284 p., 46 fig., 43 pl.

Strimple, H. L., 1972, Porosity of a fossil crinoid ossicle: Jour. Paleontology, v. 46, p. 920-921, fig. 1, 2.

Donald B. Macurda, Jr.
Museum of Paleontology
The University of Michigan
Ann Arbor, Michigan 48105

David L. Meyer
Smithsonian Tropical Research Institute
P.O. Box 2072
Balboa, Canal Zone, Panama

EXPLANATION OF PLATES

PLATE 1

Stem plates of Isocrinida.

FIGURE

1. Plan view of symplexy on internodal stem plate of *Neocrinus blakei,* ×28.

2. Plan view of synostosis on nodal stem plate of *Neocrinus blakei,* ×28.

3. Lateral view of broken interior of internodal stem plates of *Neocrinus blakei,* along axis of areola. Lumen at right, ×56.

4. Plan view of needle-like projections of stereom into lumen of a synostosis of *Endoxocrinus parrae,* ×315.

5,6. Stereo enlargement of upper center of galleried stereom of Pl. 1,*3.* Views rotated 90° to left; ×280.

PLATE 2

Stem plates of Isocrinida and Millericrinida.

FIGURE

1,2. Inclined stereo view (rotated 90°) across culmina of symplexy of an internodal of *Endoxocrinus parrae;* areola in lower left, ×77.

3. Galleried stereom in center of areola, on the symplexy of an internodal of *Endoxocrinus parrae,* ×700.

4. Synarthrial articulation of stem plate of *Democrinus* sp., ×56.

5. Lateral view of stem plate of *Democrinus* sp., ×35.

6. Fulcral ridge of synarthrial articulation of stem plate of *Democrinus* sp., ×350.

7. Enlargement of sharp grooves on fulcral ridge in Pl. 2,*6,* ×1,400.

PLATE 3

Cirri and cirral facets.

FIGURE

1,2. Inclined view of synostosis on distal surface of nodal and lateral view of cirral facet on nodal of *Endoxocrinus parrae,* ×35.

3. Inclined view of cirral of *Endoxocrinus parrae;* lower edge of plate in upper right; distal surface, ×42.

4. Enlargement of central lumen and surrounding stereom of cirral articulum of *Endoxocrinus parrae.* Upper part of plate in lower half of picture; proximal surface, ×105.

5. Proximal articular faces of cirri of *Analcidometra armata,* ×84.

6. Lateral view of cirral of *Ctenantedon kinziei,* ×70.

7. A distal cirral articulum of *Ctenantedon kinziei.* Lower edge of plate in lower half of figure, ×210.

PLATE 4

Cirral facets.

FIGURE

1,2. Stereo pair of cirral articulum on centrodorsal of *Atelecrinus balanoides* (see Pl. 5,*6*). Upper edge of centrodorsal to left, ×119.

3,4. Stereo pair of proximal articulum of proximal cirral of *Atelecrinus balanoides.* Upper edge of plate in lower left, ×84.

5,6. Stereo pair of proximal cirral articulation of *Analcidometra armata.* Lower edge of plate in lower half of view, ×210.

PLATE 5

Centrodorsal plates.

FIGURE

1,2. Oral and lateral views of centrodorsal plate of *Analcidometra armata,* ×49.

3. Stereomic microstructure in center of cavity on ventral surface of *Analcidometra armata* (see Pl. 5,*1*), ×490.

4. Stereomic microstructure in center of cavity on ventral surface of *Nemaster rubiginosa,* ×140.

5,6. Inclined oral and lateral views of centrodorsal of *Atelecrinus balanoides,* ×28.

PLATE 6

Centrodorsal-basal suture of *Atelecrinus.*

FIGURE

1,2. Oral stereo view of upper surface of centrodorsal of *Atelecrinus balanoides,* centered on middle of contact with overlying basal; lumen of centrodorsal in upper right, ×91.

3,4. Lower surface of basal of *Atelecrinus balanoides* that is in contact with surface of centrodorsal in Pl. 6,*1,2,* ×70.

5,6. Aboral view of basals of *Atelecrinus balanoides;* single plate outlined on right by electronic charging, ×28.

PLATE 7

Basal plates.

FIGURE

1,2. Aboral stereo view of stem articulum on lower surface of basal of *Endoxocrinus parrae,* ×28.

3,4. Stereo view of inner edge of basal plate of *Endoxocrinus parrae,* showing part of concavity for main aboral nerve center (right) and its continuation aborally (left) toward the stem facet, ×28.

5. View of upper (distal) surface of basal of *Neocrinus blakei,* with external surface on left and two nerve canals on right, ×28; compare with Pl. 7,*7,8.*

6. Lateral view of calyx (basals right and radials left) of *Democrinus* sp., ×22.

7,8. Stereo view of inner edge of basal plate of *Neocrinus blakei,* with stem articulum on lower edge. Main aboral nerve center in concavity in lower half; nerves bifurcate in plate to come out through two openings on upper surface (Pl. 7,5), ×70; compare with Pl. 7,*3,4.*

PLATE 8

Nerve canals.

FIGURE

1,2. Stereo view of oral surface of *Comactinia echinoptera* var. *meridionalis* with two basal rays still in position. Latter form cover for concavity of main aboral nerve center in centrodorsal. Outer openings contain nerve canals which lead to adjacent overlying radials, ×56.

3,4. Stereo view of fractured interior of calyx of *Democrinus* sp. showing internal space for chambered organ and main aboral nerve center and continuation of nerve canals outward (left) toward radial facets, ×35; orientation as in Pl. 7,*6.*

5,6. Stereo view of lateral edge of radial (center of figure) of *Analcidometra armata* from an interior and slightly below vantage; back edges of lobes of muscular facets in upper left. Opening in right center for horizontal nerve ring through radials; opening to its right for nerve canal from main aboral nerve center to radial facet; both junction internally, ×98.

PLATE 9

Radials.

FIGURE

1. Oral view of upper surface of radial of *Analcidometra armata;* radial facet in upper left, ×98.

2. View of lateral surface of radial of *Nemaster rubiginosa,* with lateral nerve canal at left and groove where upper surface of basal ray fits at base, ×35.

3,4. Stereo enlargement of ridges on upper edge of lateral surface of radial of *Nemaster rubiginosa,* Pl. 9,*2,* ×140.

5,6. Stereo view of frontal (internal) edge of radial of *Nemaster rubiginosa* with horizontal nerve canal opening out laterally and nerve canals from centrodorsal and basal rays centrally located, ×35.

PLATE 10

Muscular articulations of *Endoxocrinus.*

FIGURE

1,2. Inclined oral stereo view of distal muscular articulum of brachial of *Endoxocrinus parrae* with pinnular articulum in lower left, ×35.

3,4. Stereo view of intermuscular furrow between muscle fossae on brachial of *Endoxocrinus parrae,* ×105.

5,6. Stereo view of transition from muscle fossa (left) to interarticular ligament fossa (right) on brachial of *Endoxocrinus parrae,* ×350.

PLATE 11

Muscular articulation of *Endoxocrinus.*

FIGURE

1. Detail of stereom in dorsal ligament fossa of radial of *Endoxocrinus parrae,* ×560.

2. Muscular articulation on radial of *Endoxocrinus parrae,* ×35.

3,4. Stereo view of dorsal ligament fossa (lower), fulcral ridge, and interarticular ligament fossa (upper) on primibrachial of *Endoxocrinus parrae,* ×105.

5,6. Stereo view of stereomic microstructure in muscle fossa on radial of *Endoxocrinus parrae,* ×315.

PLATE 12

Muscular articulation of *Neocrinus.*

FIGURE

1,2. Inclined oral stereo view of distal muscular articulum of brachial of *Neocrinus blakei* with pinnular articulum in upper center, ×35.

3,4. Inclined view of upper edge of muscle fossa of brachial of *Neocrinus blakei* such as that of left center of Pl. 12,*1,2,* ×315.

5,6. Stereo view of transition from muscle fossa (left) to interarticular ligament fossa (right) on primibrachial of *Endoxocrinus parrae,* ×350.

PLATE 13

Radials of *Democrinus.*

FIGURE

1. Oral view of muscular articula on radials of *Democrinus* sp., ×28.

2. View of interarticular ligament fossa (lower), muscle fossa (center) and its bordering wall (upper) on radial of *Democrinus* sp., ×280; compare with Pl. 13,*3,4.*

3,4. Inclined stereo view of muscular articulum on radial of *Democrinus* sp., ×56.

5,6. Inclined stereo lateral view of muscular articulation of *Democrinus* sp. with dorsal ligament fossa and pit (lower), fulcral ridge, lumen of nerve canal (center) bordered by fossae of interarticular ligaments and muscle fossae (upper), ×175.

PLATE 14

Brachials of *Democrinus.*

FIGURE

1,2. Stereo view of muscular articulum on proximal surface of first brachial of *Democrinus* sp., ×63.

3,4. Stereo view of transition from muscle fossa (left) to interarticular ligament fossa (right) on first brachial of *Democrinus* sp., ×315.

5. Inclined oral view of a proximal brachial plate of *Democrinus* sp., ×56.

6. Inclined view of trifascial synarthry on distal surface of first brachial of *Democrinus* sp., ×70.

PLATE 15

Synarthry of *Democrinus* and muscular articulation of *Nemaster.*

FIGURE

1,2. Detailed stereo view of trifascial synarthry on distal surface of first brachial of *Democrinus* sp., ×140.

3,4. Inclined oral stereo view of distal muscular articulum of brachial of *Nemaster rubiginosa* with pinnular articulum in lower left, ×28.

5,6. Stereo view of transition from muscle fossa (upper right) to interarticular ligament fossa (lower left) on brachial of *Nemaster rubiginosa,* ×1,050.

PLATE 16

Muscular articulations of *Nemaster* and *Analcidometra.*

FIGURE

1. Fulcral ridge of muscular articulation of primibrachial of *Nemaster rubiginosa* with dorsal ligament fossa (below) and interarticular ligament fossa (above), ×210.

2. Enlargement of fulcral ridge of Pl. 16,*1*, showing signs of abrasive wear, ×700.

3,4. Muscular articulum of brachial of *Analcidometra armata* and an enlargement of its dorsal ligament fossa, ×91 and ×280.

5,6. Stereo view of transition from muscle fossa (upper left) to interarticular ligament fossa (upper center) of *Analcidometra armata;* dorsal ligament fossa in lower right, ×245.

PLATE 17

Brachials of *Analcidometra, Atelecrinus,* and *Ctenantedon.*

FIGURE

1,2. Oral stereo view of brachial of *Analcidometra armata* with pinnular facet in upper left, ×84.

3,4. Stereo view of muscular articulum on brachial of *Ctenantedon kinziei,* ×84.

5,6. Stereo view of transition from muscle fossa (upper left) to interarticular ligament fossa (lower right) on brachial of *Ctenantedon kinziei,* ×420.

7,8. Lateral stereo view of ridged process on primibrachial of *Atelecrinus balanoides,* ×30; compare with Pl. 18, *3,4.*

PLATE 18

Muscular articulations of *Atelecrinus* and *Crinometra.*

FIGURE

1. Muscular articulum on brachial of *Crinometra brevipinna,* ×28.

2. Enlargement of left center of Pl. 18,*1*, showing transition from muscle fossa (upper left) to interarticular ligament fossa (lower), ×245.

3,4. Stereo view of muscular articulum on primibrachial of *Atelecrinus balanoides,* with ridged process in upper left (see Pl. 17,*7,8*), ×28.

5,6. Stereo view of transition from muscle fossa (upper left) to interarticular ligament fossa (lower right) on primibrachial of *Atelecrinus balanoides,* ×700.

PLATE 19

Muscular articulation of *Atelecrinus* and syzygy of *Nemaster.*

FIGURE

1. Fulcral ridge and ligament fossae of muscular articulum of primibrachial of *Atelecrinus balanoides* (see lower center of Pl. 18,*3,4*), ×210.

2. Syzygy on epizygal of *Nemaster rubiginosa,* ×28.

3,4. Stereo view of culmina at outer edge of syzygy of *Nemaster rubiginosa,* ×280.

5. Detail of culmina in Pl. 19,*3,4,* ×1,050.

6. Culmina near central lumen on syzygy of brachial of *Nemaster rubiginosa,* ×210.

PLATE 20

Syzygies of *Analcidometra, Atelecrinus,* and *Ctenantedon.*

FIGURE

1,2. Stereo view of culmina around central lumen on brachial syzygy of *Ctenantedon kinziei,* ×84.

3,4. Stereo view of syzygy on proximal surface of axillary primibrachial of *Analcidometra armata,* ×140.

5,6. Syzygy of brachial of *Atelecrinus balanoides* and detailed view of left center adjacent to central lumen, ×28 and ×455.

PLATE 21

Synarthries.

FIGURE

1,2. Synarthry on brachial of *Comactinia echinoptera* var. *valida* and enlargement of upper ridge, ×28 and ×175.

3. Synarthry on proximal surface of axillary primibrachial of *Analcidometra armata,* ×105.

4. Synarthry on distal surface of first primibrachial of *Neocrinus blakei,* ×28.

5,6. Stereo view of synarthry of brachial of *Atelecrinus balanoides,* ×42.

PLATE 22

Symmorphy.

FIGURE

1,2. Stereo view of symmorphy on hypozygal brachial of *Neocrinus blakei,* ×35.

3,4. Stereo view of symmorphy on epizygal brachial of *Neocrinus blakei,* ×35.

5. Enlarged view of culmina in symmorphy on lower edge of hypozygal of *Neocrinus blakei,* ×140.

6. Lower edge of articulum on proximal surface of axillary primibrachial of *Endoxocrinus parrae* (see Pl. 23,*1*), ×35.

PLATE 23

Brachial surfaces.

FIGURE

1. Lower left edge of articulum on proximal surface of axillary primibrachial of *Endoxocrinus parrae* (see Pl. 22,*6*), ×70.

2. Exterior surface of brachial of *Endoxocrinus parrae,* ×350.

3. Exterior surface of primibrachial of *Nemaster rubiginosa,* ×315.

4. Exterior surface of brachial of *Comactinia echinoptera* var. *valida,* ×210.

5,6. Stereo view of upper surface of brachial of *Endoxocrinus parrae,* with pinnular facet lower left, proximal direction at top (see Pl. 10,*1,2*), ×70.

PLATE 24

Pinnulars and facets of *Endoxocrinus.*

FIGURE

1,2. Stereo view of pinnular articulum on brachial of *Endoxocrinus parrae;* compare with Pl. 10,*1,2* and Pl. 23,*5,6.* Lower right is adoral direction of brachial, ×112.

3,4. Stereo view of asymmetrical proximal articulum of the proximal pinnular of *Endoxocrinus parrae,* ×56.

5,6. Inclined oral stereo view of pinnular of *Endoxocrinus parrae,* ×70.

PLATE 25

Pinnulars of *Endoxocrinus* and pinnular facet of *Neocrinus.*

FIGURE

1. Broken pinnular of *Endoxocrinus parrae* showing stereom of central nerve canal, ×140.

2. Muscular articulum of median or distal pinnular of *Endoxocrinus parrae;* upper left edge of plate is the inner side, ×70.

3,4. Enlarged stereo view of muscular articulum of *Endoxocrinus parrae* in Pl. 25,*2* (view rotated 90° to left), ×210.

5,6. Stereo view of pinnular articulum on brachial of *Neocrinus blakei;* compare with Pl. 12,*1,2;* adoral direction is to lower left, ×84.

PLATE 26

Pinnulars and facets of *Democrinus.*

FIGURE

1,2. Inclined oral stereo view of brachial and pinnular facet (upper right) of *Democrinus* sp. from distal vantage point, ×91.

3,4. Stereo view of asymmetrical muscular articulum on proximal surface of the proximal pinnular of *Democrinus* sp., ×175.

5,6. Inclined stereo view of proximal end of second pinnular of *Democrinus* sp., ×245.

PLATE 27

Pinnulars of *Democrinus* and pinnular facet of *Nemaster.*

FIGURE

1,2. Oral stereo view of median or distal pinnular of *Democrinus* sp., ×147.

3,4. Stereo view of articulum on median or distal pinnular of *Democrinus* sp., ×560.

5,6. Stereo view of upper half of pinnular articulum on brachial of *Nemaster rubiginosa,* ×210; compare with Pl. 15,*3,4.*

PLATE 28

Pinnulars of *Nemaster.*

FIGURE

1,2. Stereo view of asymmetrical muscular articulum on proximal surface of the proximal pinnular of *Nemaster rubiginosa,* ×98.

3. Inclined lateral view of pinnular of *Nemaster rubiginosa;* proximal surface in upper right, ×140.

4,5. Oral view of pinnular of *Nemaster rubiginosa* and an enlargement of lower center; proximal end at top, ×77 and ×315.

6,7. Stereo view of muscular articulum on distal surface of a pinnular of *Nemaster rubiginosa;* upper surface at top, ×140.

PLATE 29

Pinnulars and pinnular facets of *Comactinia.*

FIGURE

1,2. Stereo view of pinnular articulum on brachial of *Comactinia echinoptera* var. *valida;* trough of upper surface of brachial at extreme left, ×210.

3,4. Stereo view of muscular articulum on proximal surface of pinnular of *Comactinia echinoptera* var. *valida;* upper surface at top, ×105.

5. Enlargement of spines on pinnular *Comactinia echinoptera* var. *valida* in Pl. 29,*3,4,* ×315.

6. A lateral view of a distal pinnular of *Comactinia echinoptera* var. *valida;* spines on base, ×175.

PLATE 30

Pinnulars and pinnular facets of *Comactinia* and *Analcidometra.*

FIGURE

1. Oral view of pinnular of *Comactinia echinoptera* var. *valida,* with proximal end at top, ×105.

2. Pinnular articulum on brachial of *Analcidometra armata,* adoral direction to right, ×205. Compare with Pl. 17,*1,2.*

3. Inclined oral view of pinnular of *Comactinia echinoptera* var. *valida,* with oral surface facing lower right and adoral end in lower left, ×140.

4. Enlargement of central part of pinnular articulum on brachial of *Analcidometra armata* in Pl. 17,*1,2,* central lumen in upper center, ×525.

5,6. Stereo view of asymmetrical muscular articulum on proximal surface of the proximal pinnular of *Analcidometra armata,* ×182.

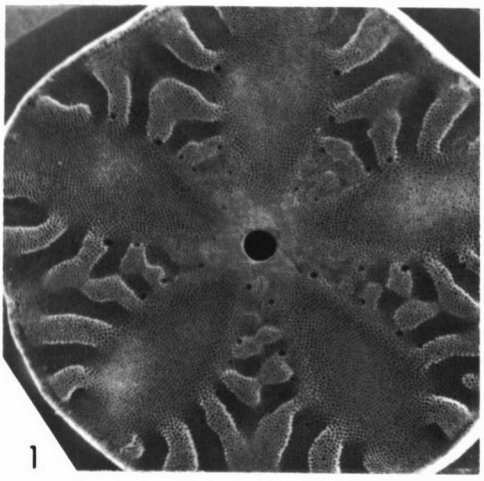
1

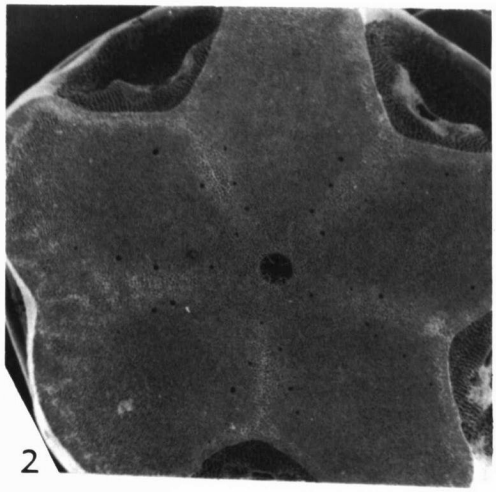
2


3

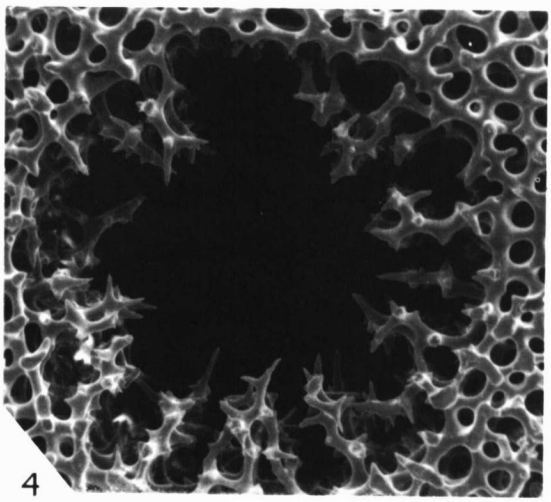
4

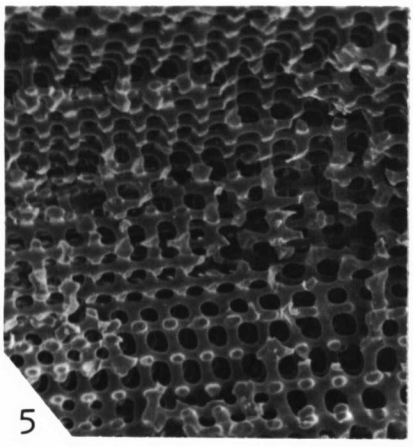
5

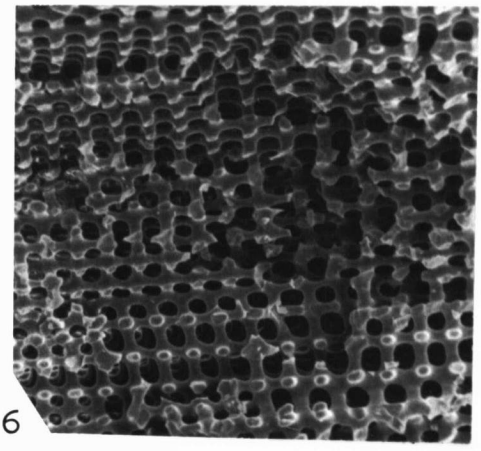
6

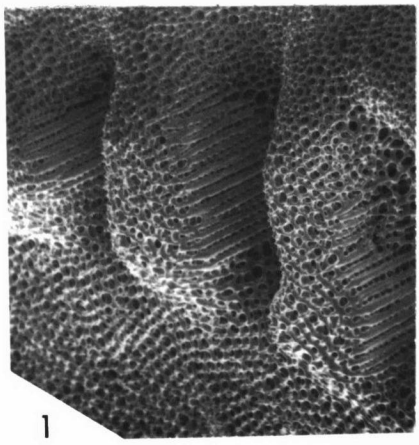
1

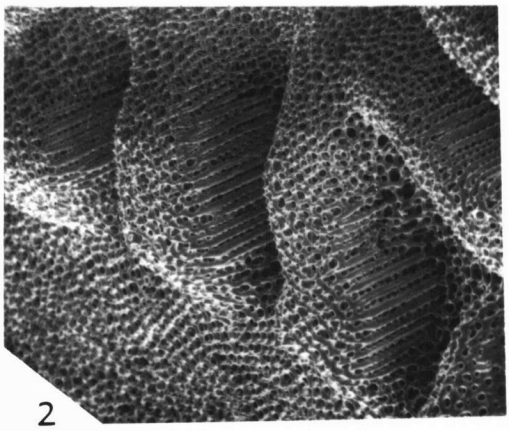
2

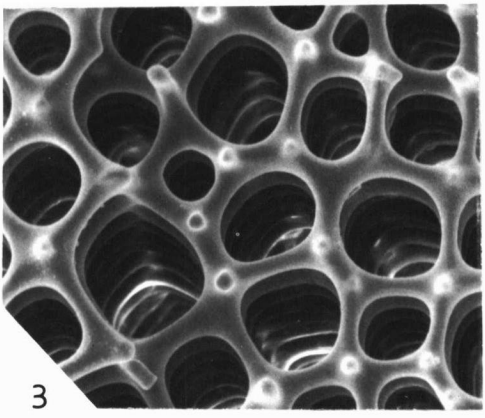
3

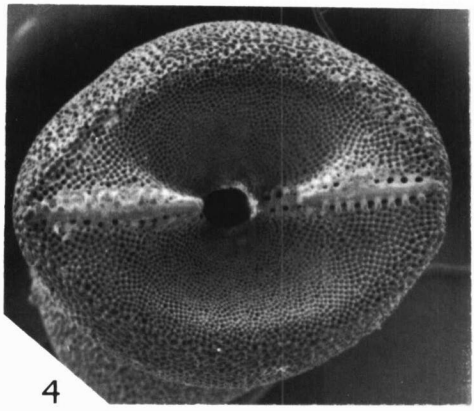
4

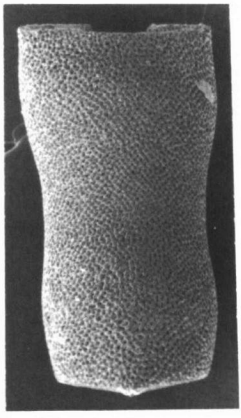
5

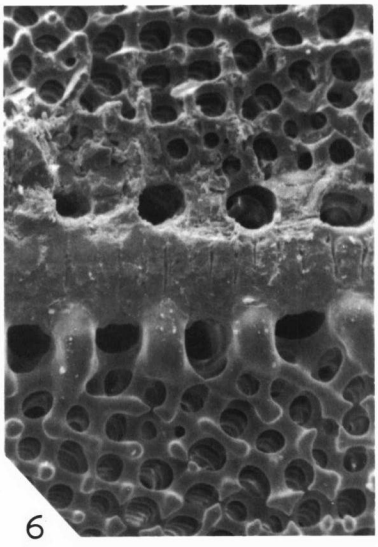
6


7

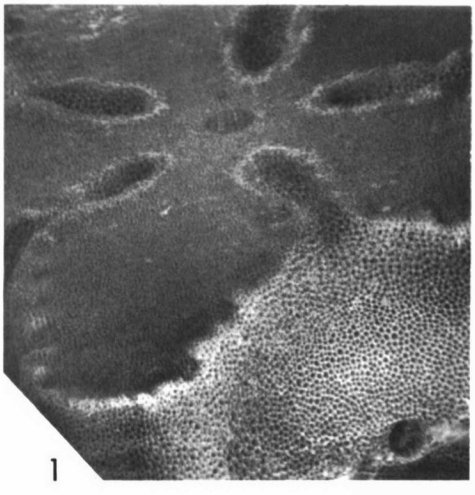

1

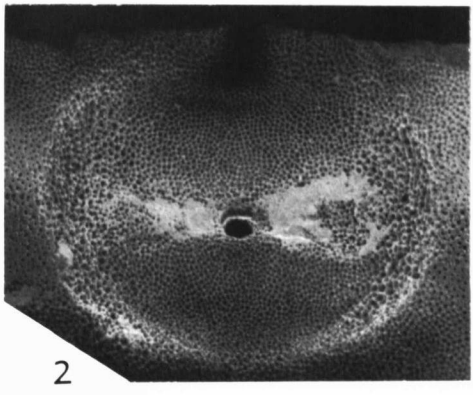

2

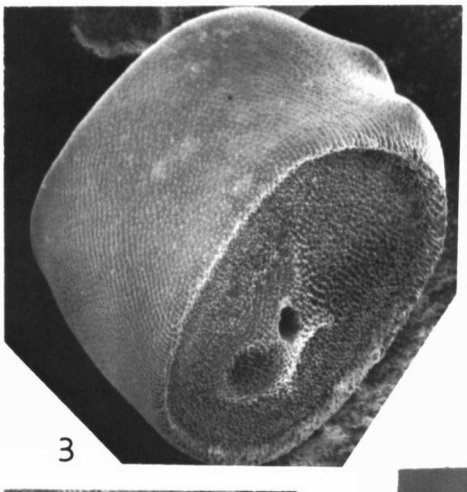

3

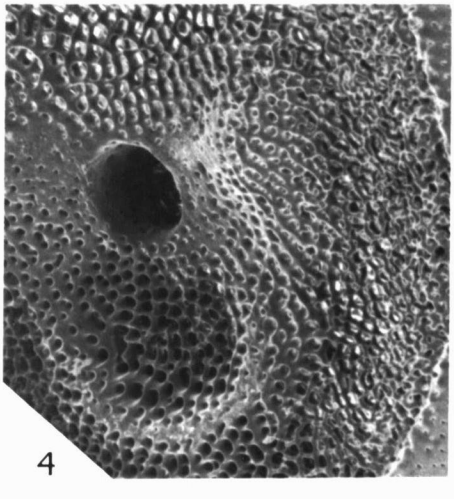

4

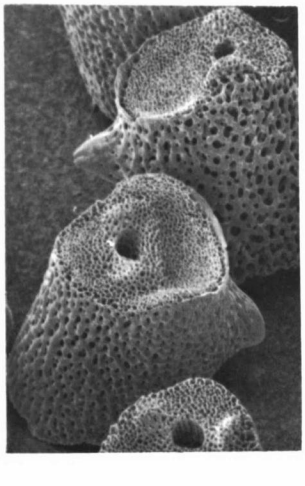

5

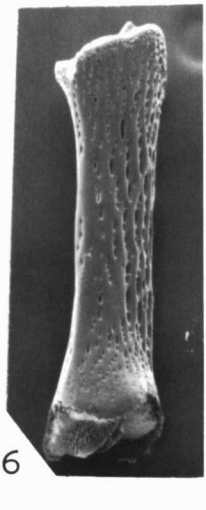

6

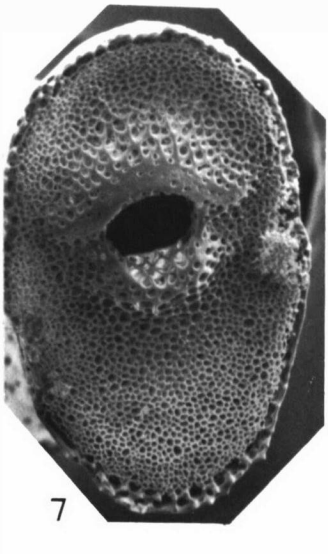

7

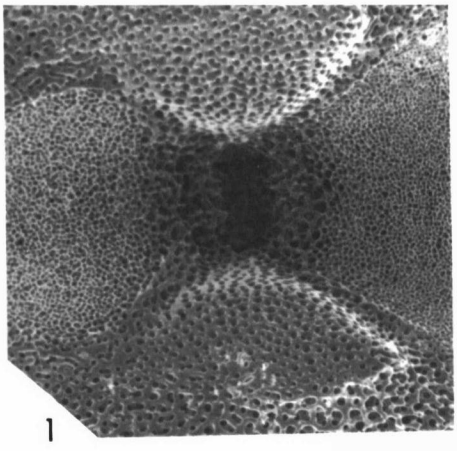
1

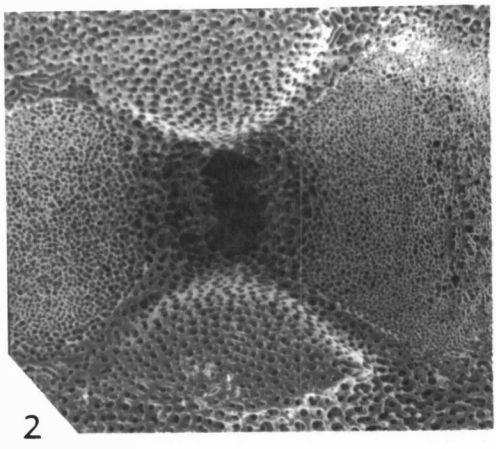
2

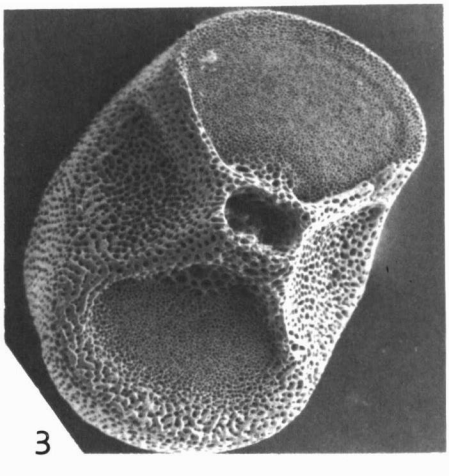
3

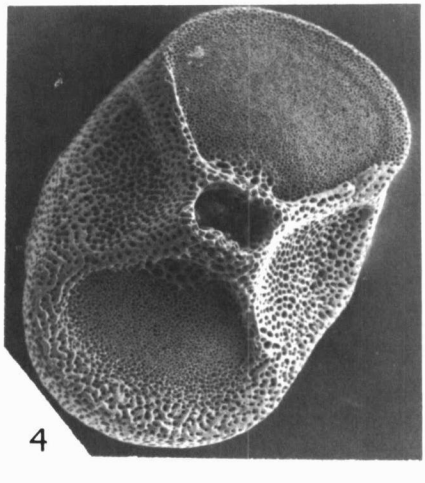
4

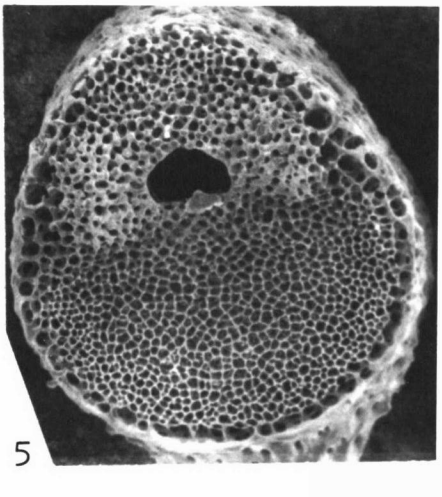
5

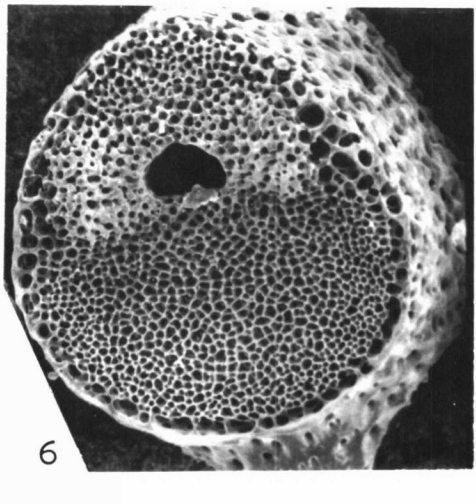
6

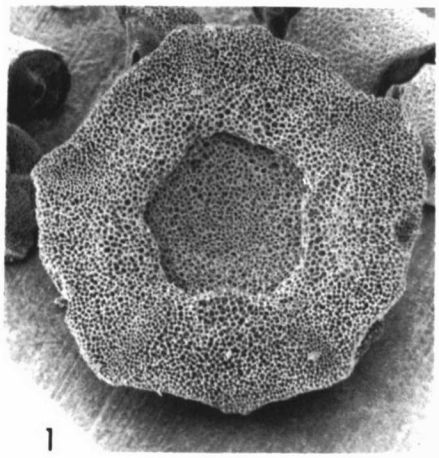
1

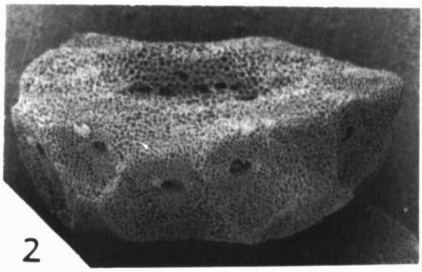
2

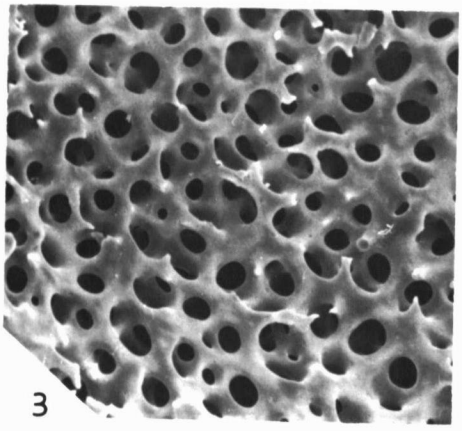
3

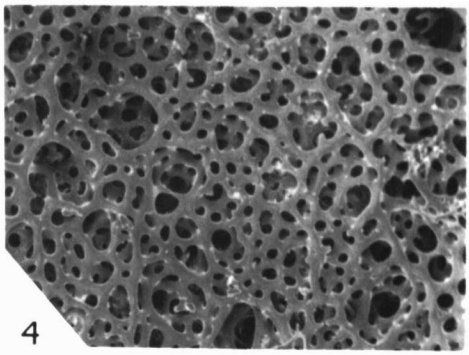
4

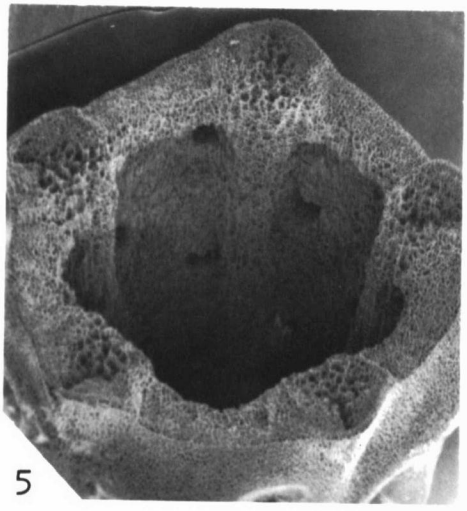
5

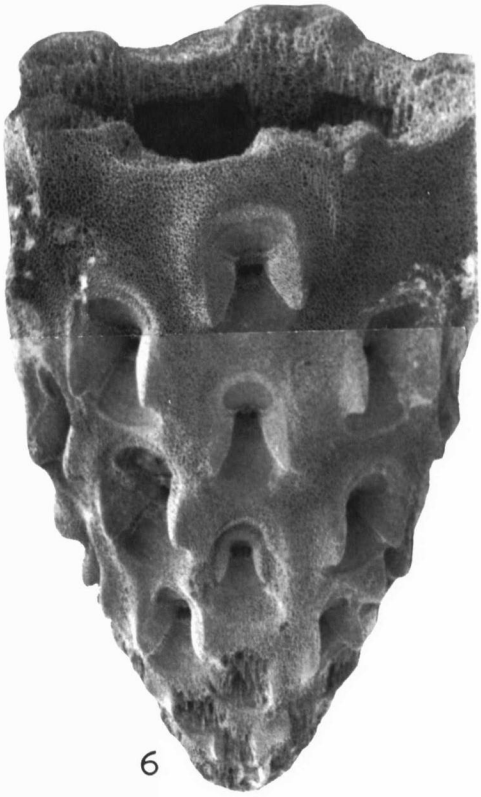
6

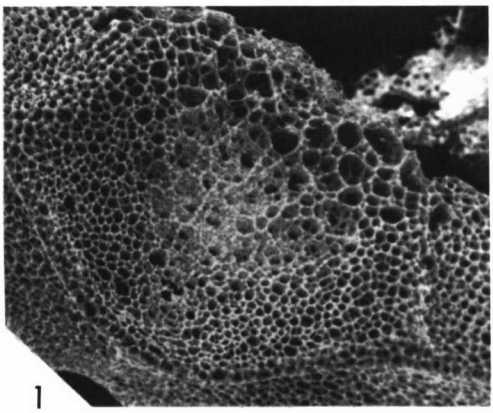
1

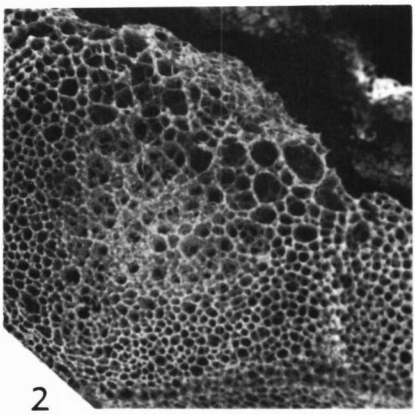
2

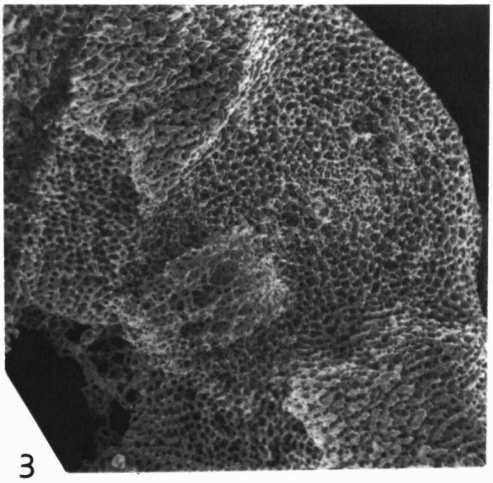
3

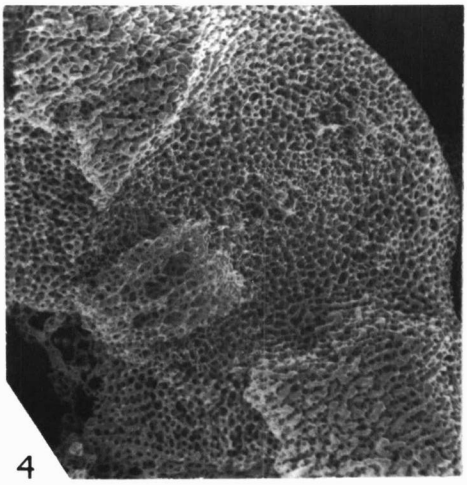
4

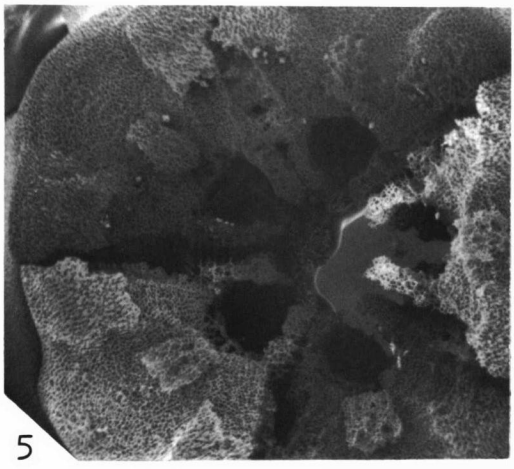
5

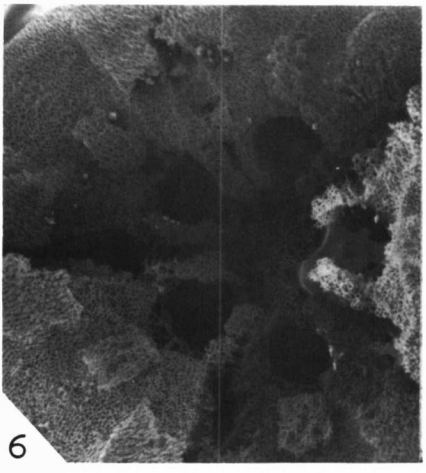
6

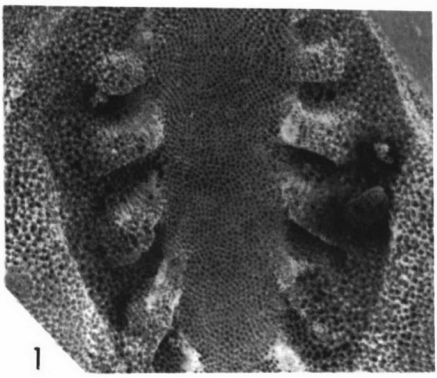
1

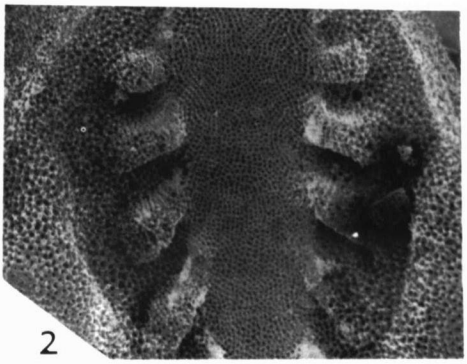
2

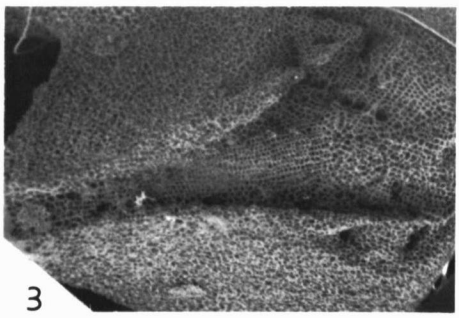
3

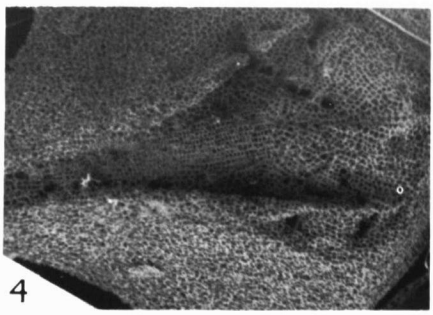
4

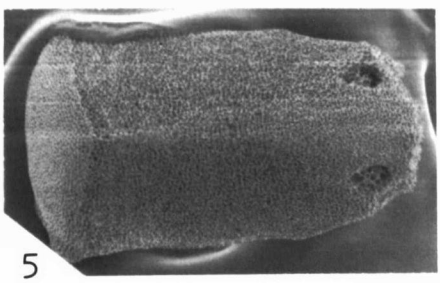
5


6

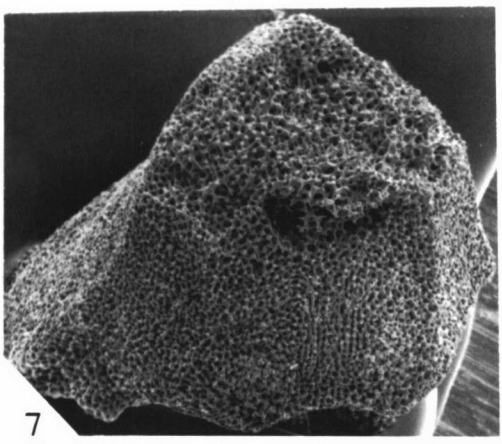
7

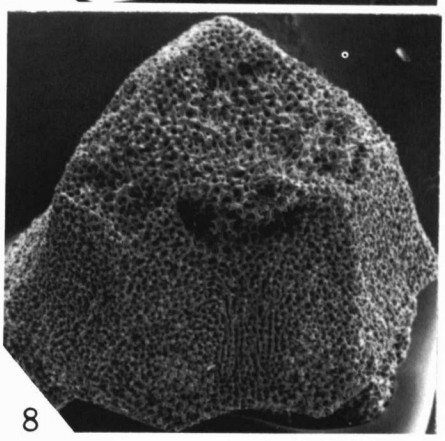
8

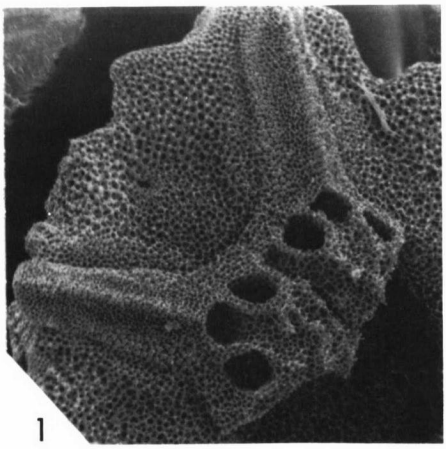
1

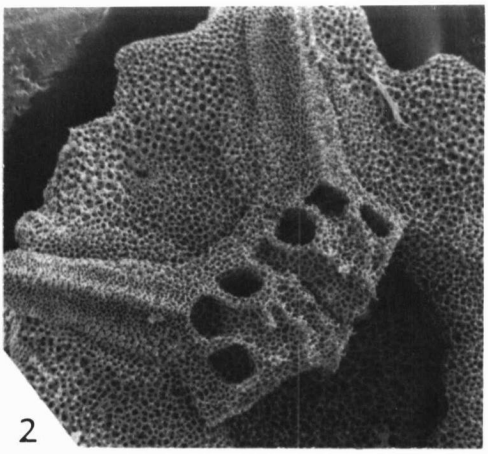
2

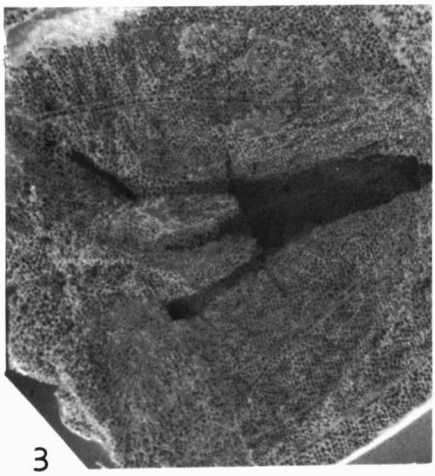
3

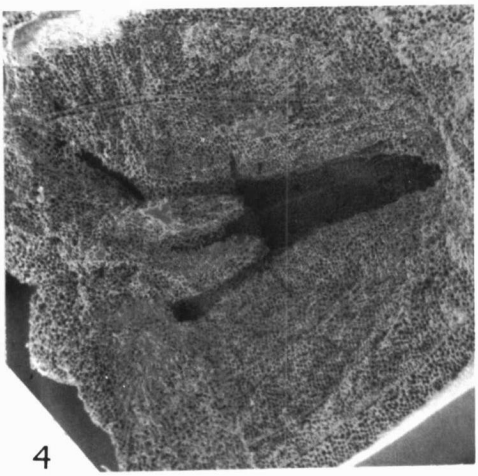
4

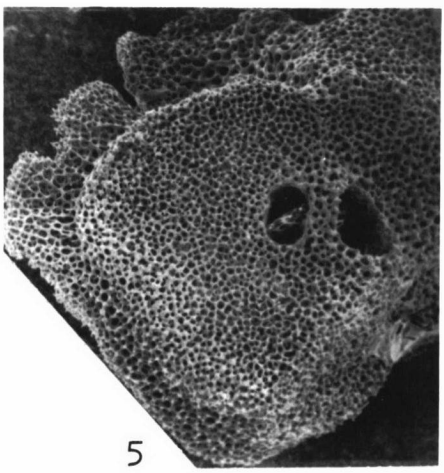
5

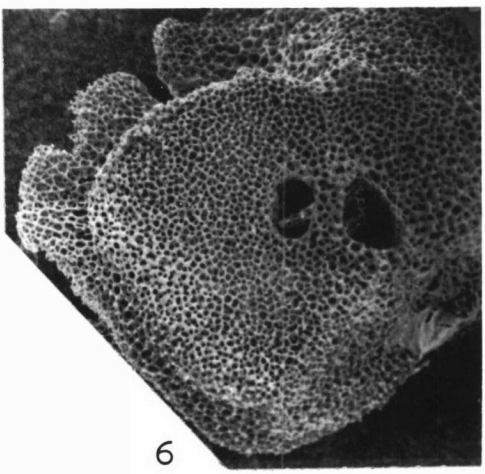
6

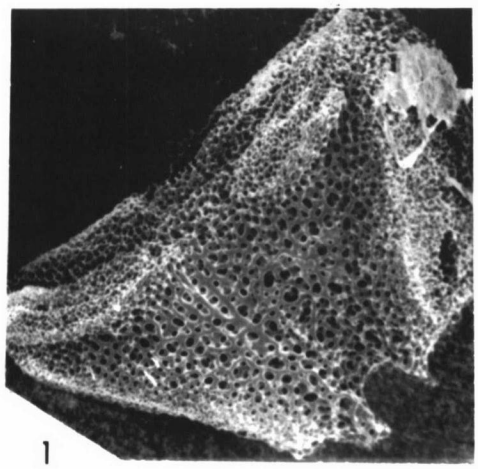
1

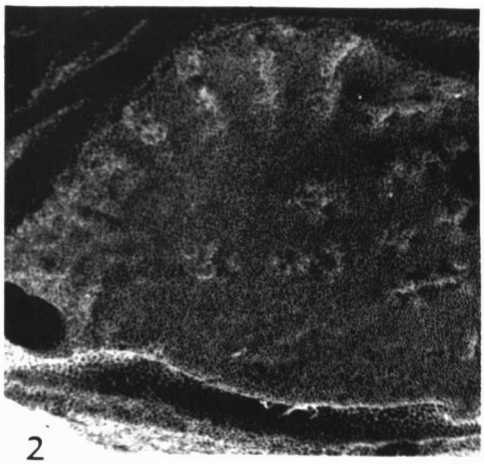
2

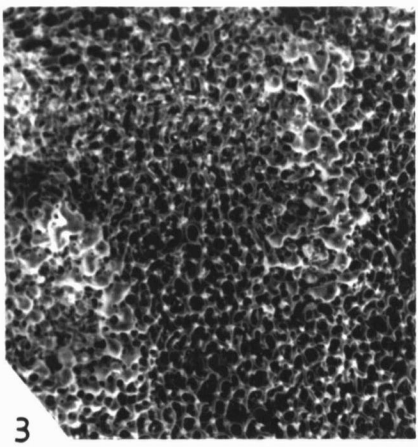
3

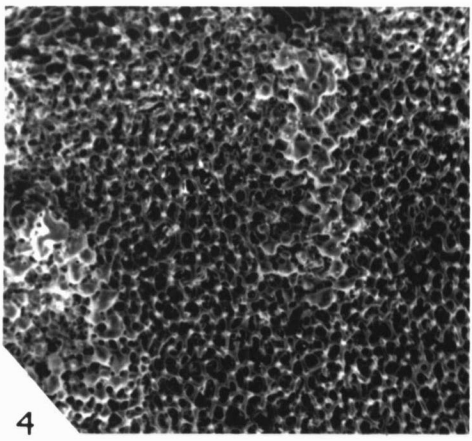
4

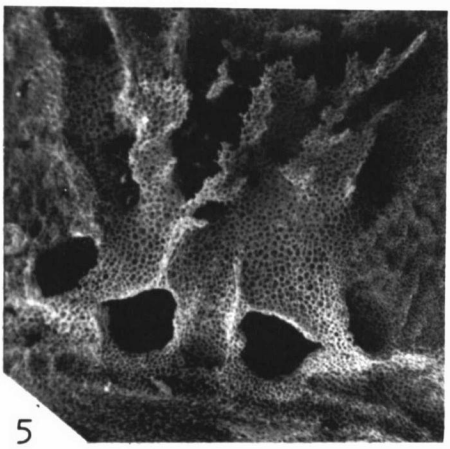
5

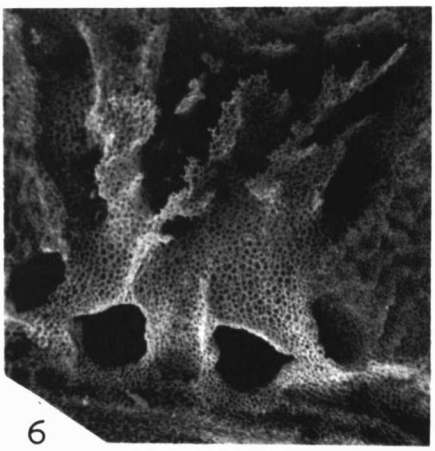
6

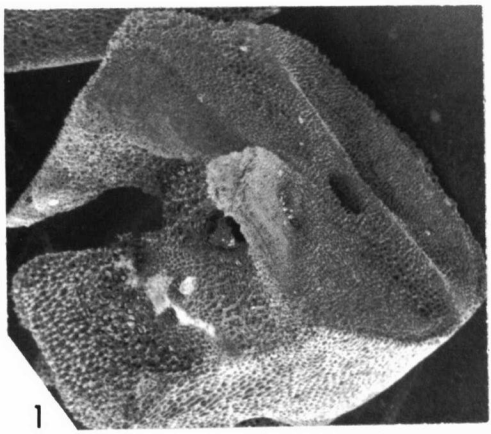
1

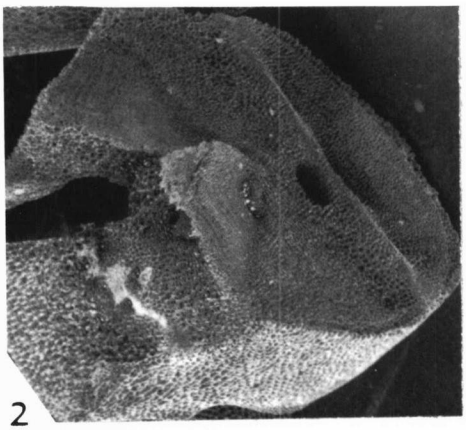
2

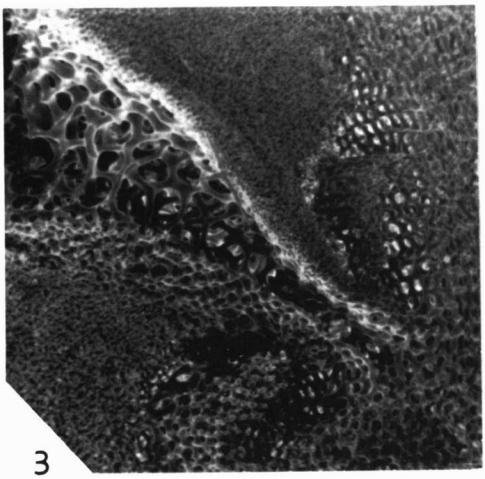
3

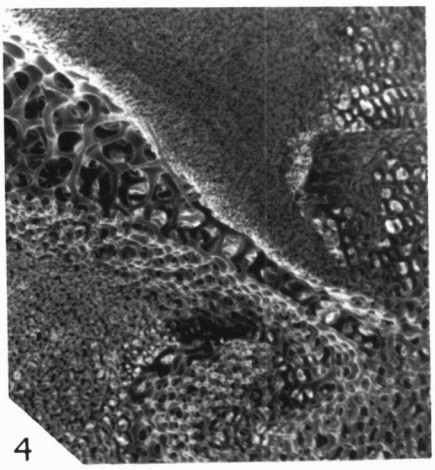
4

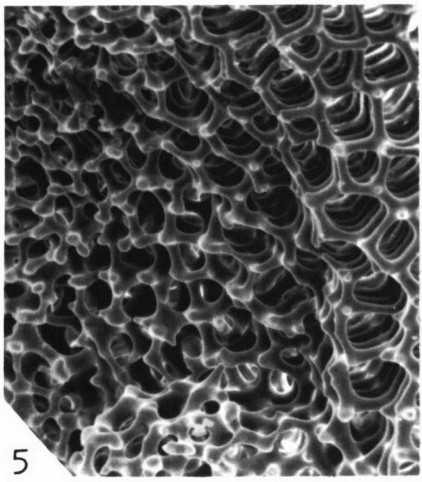
5

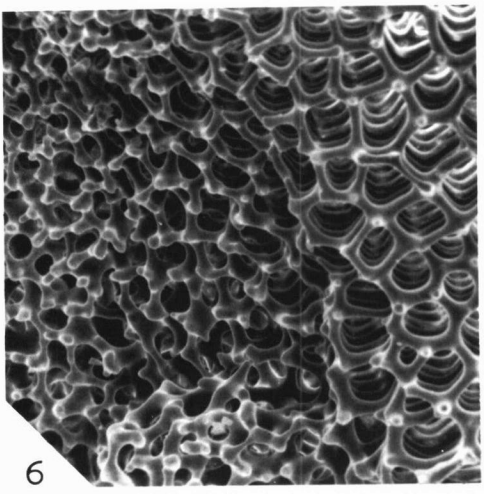
6

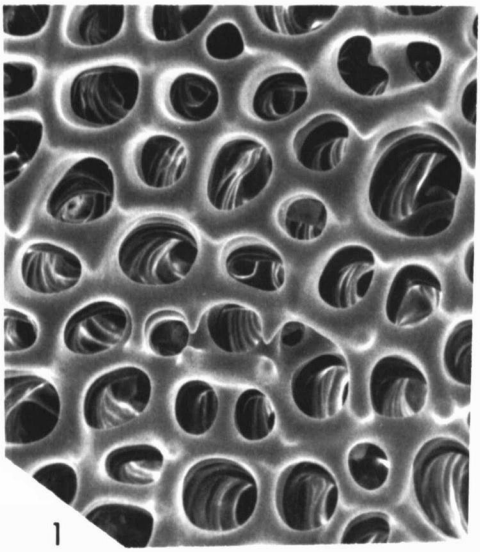
1

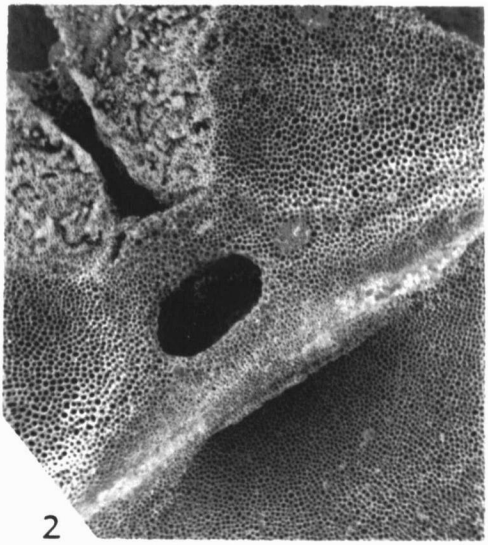
2

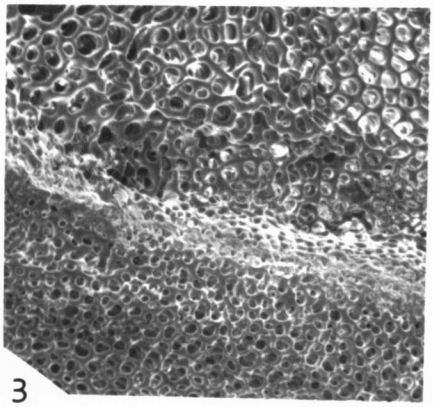
3

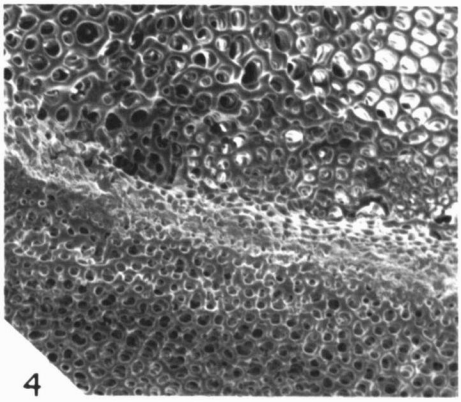
4

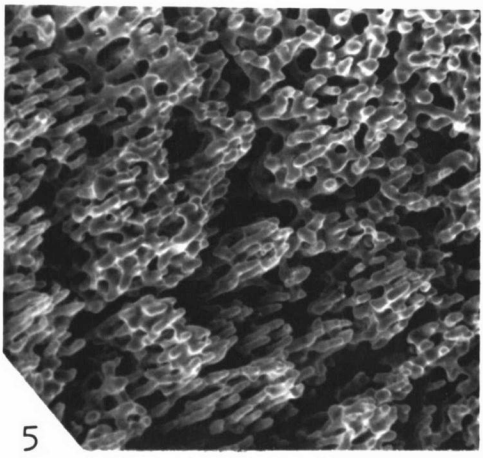
5

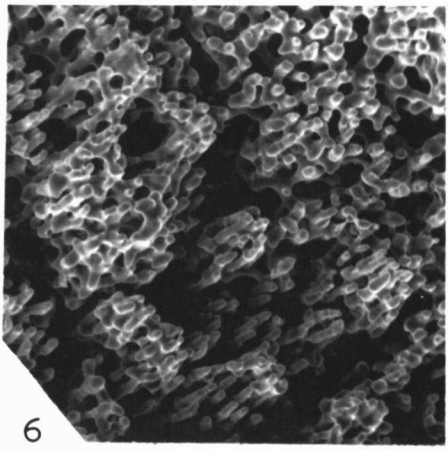
6

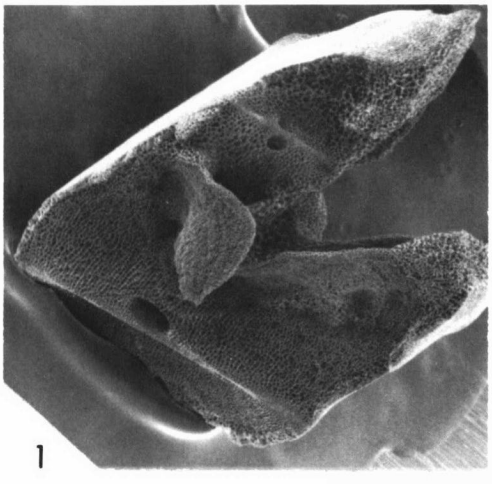
1

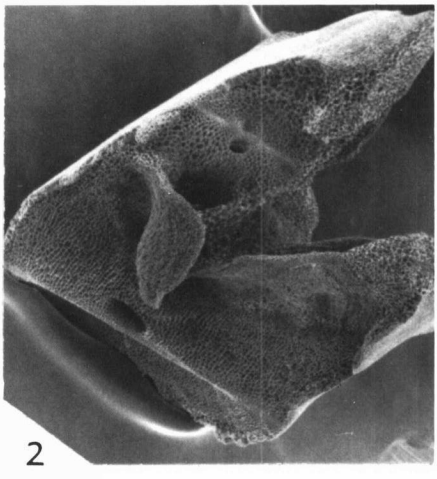
2

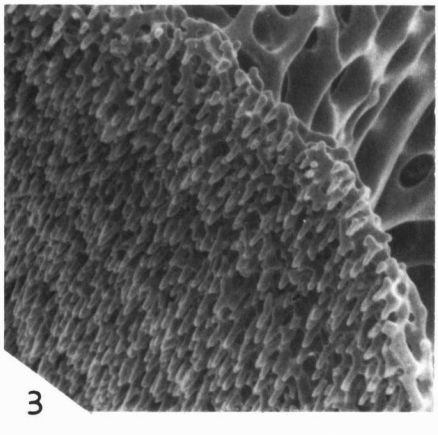
3

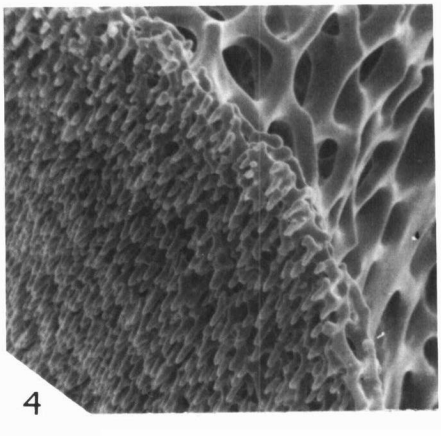
4

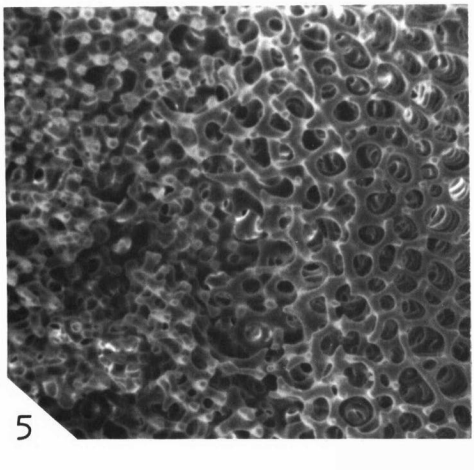
5

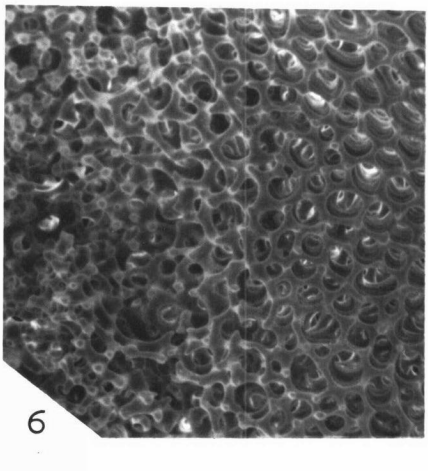
6

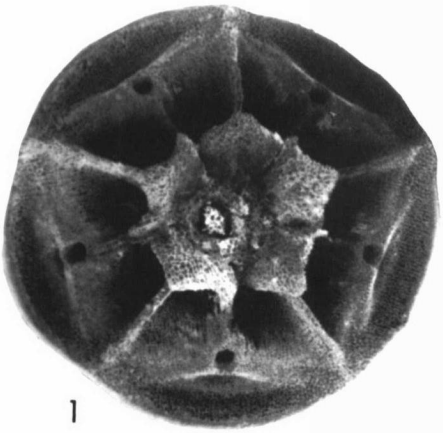

1

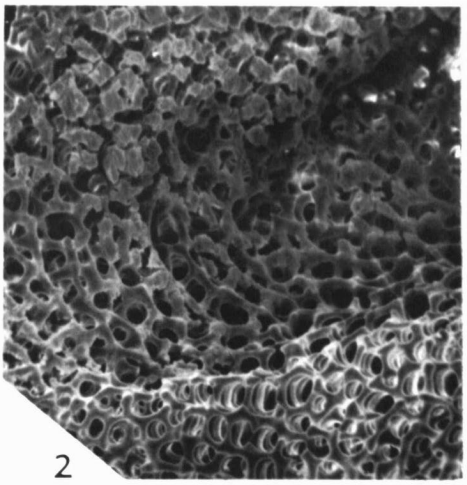

2

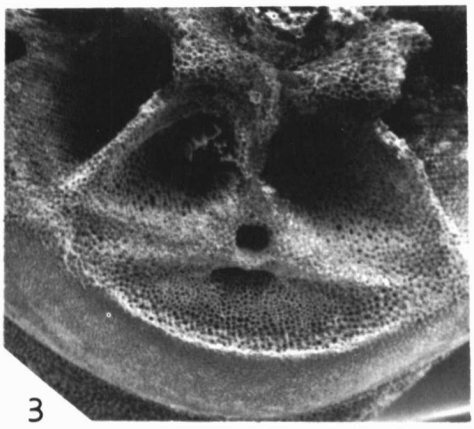

3

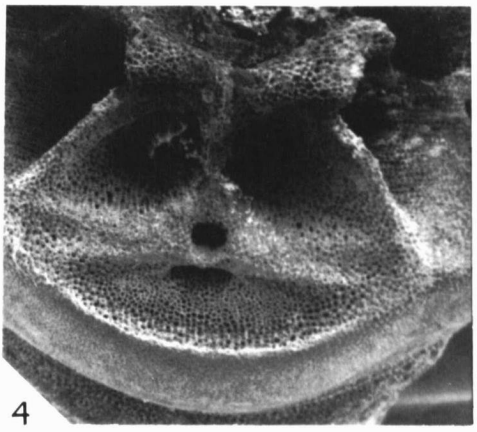

4

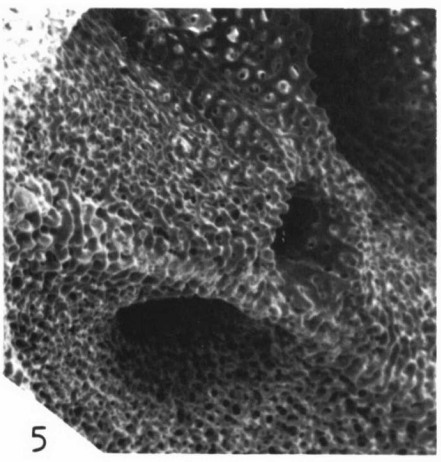

5

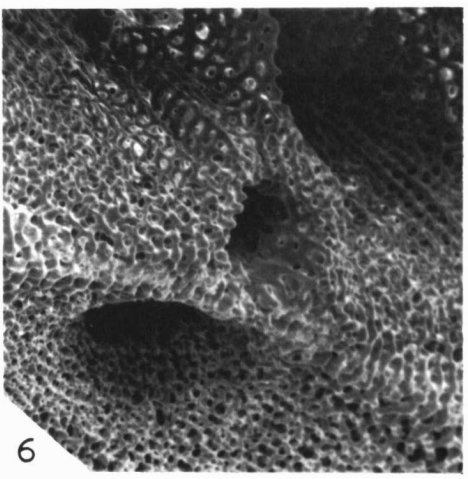

6

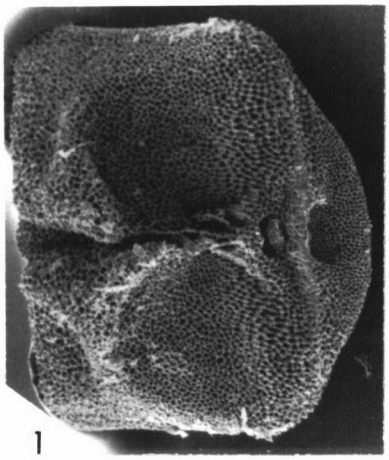

1

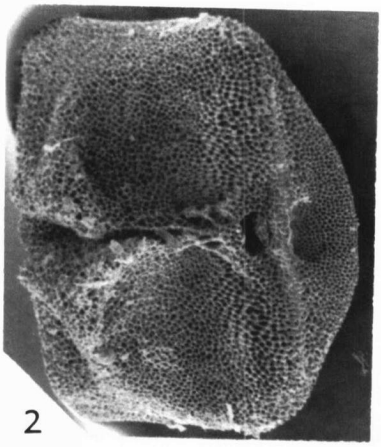

2

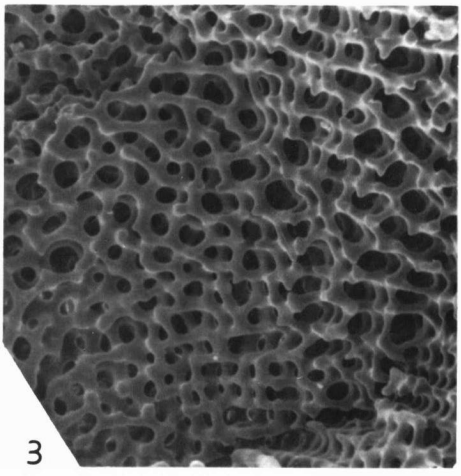

3

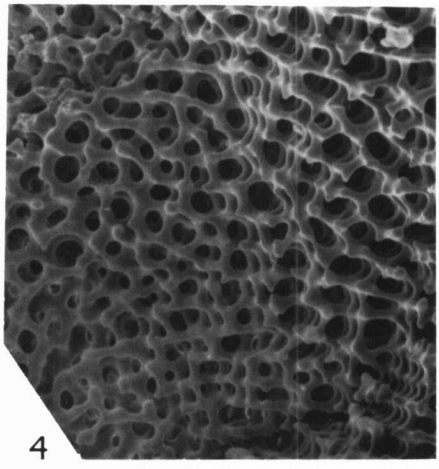

4

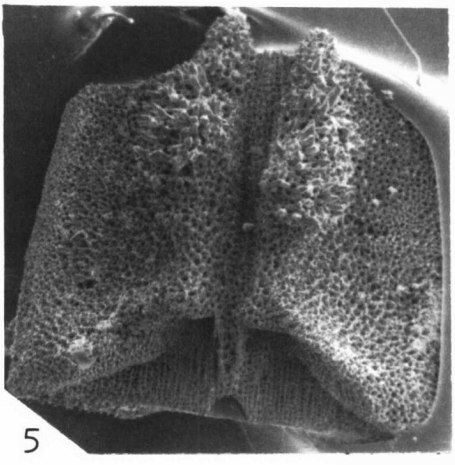

5

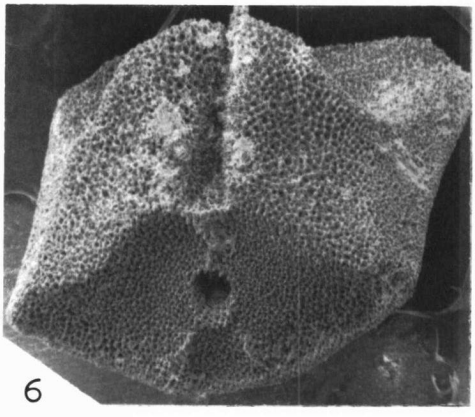

6

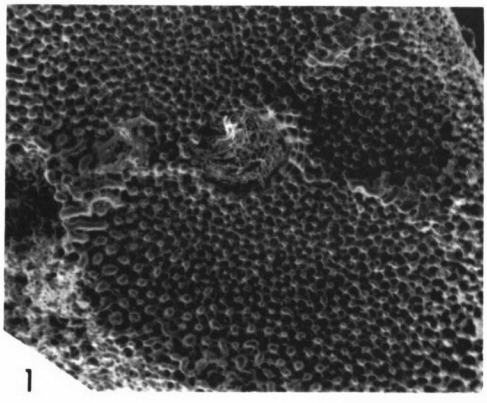
1

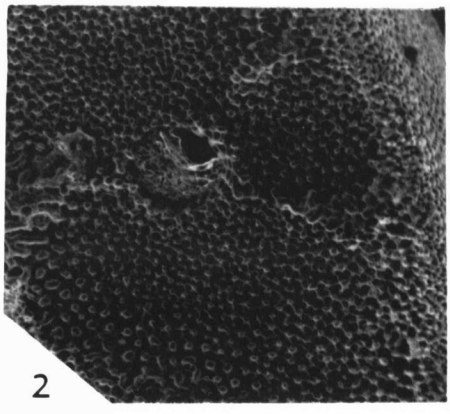
2

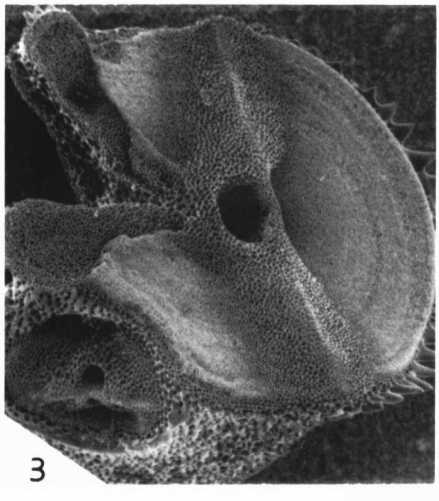
3

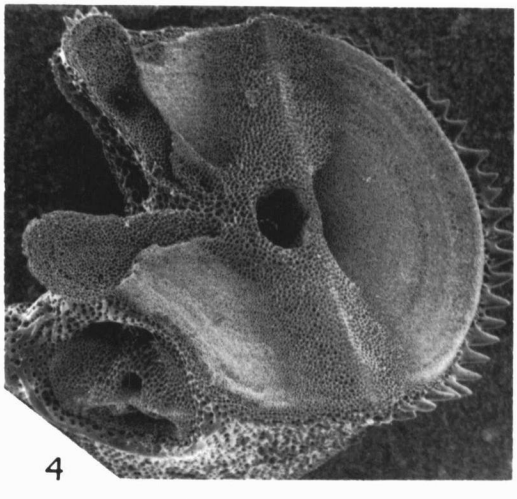
4

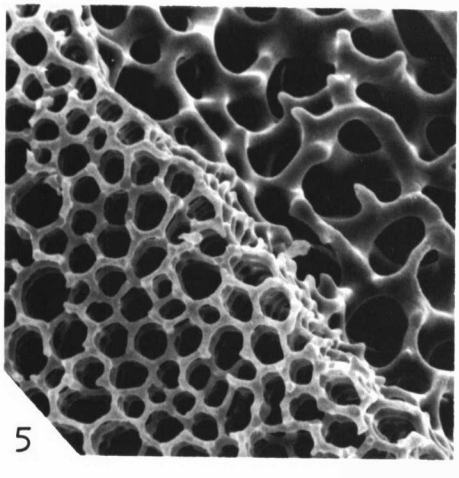
5

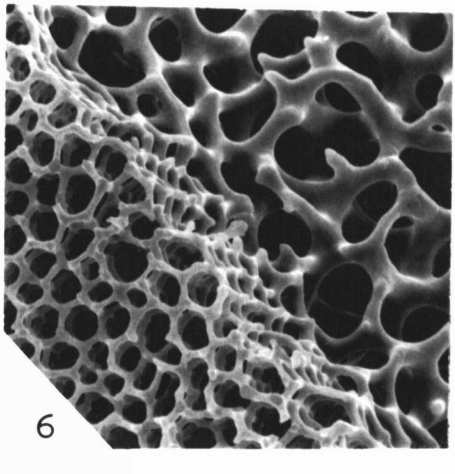
6

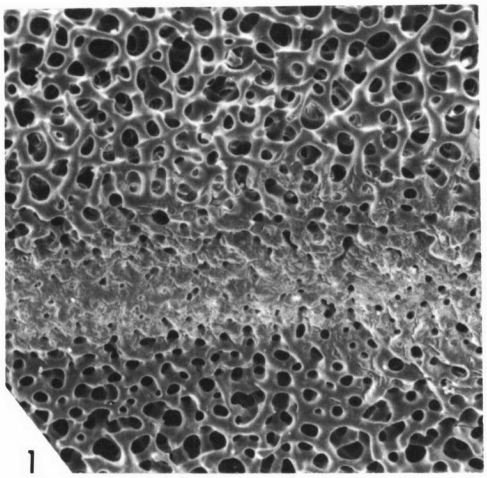
1

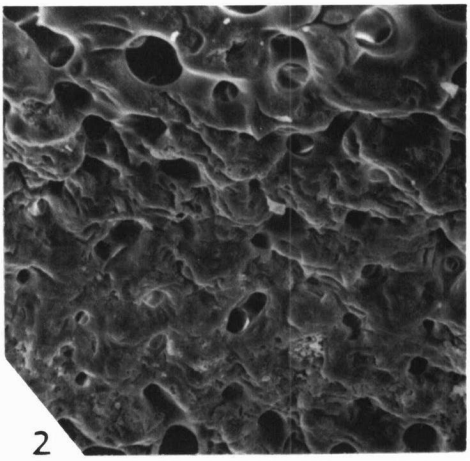
2

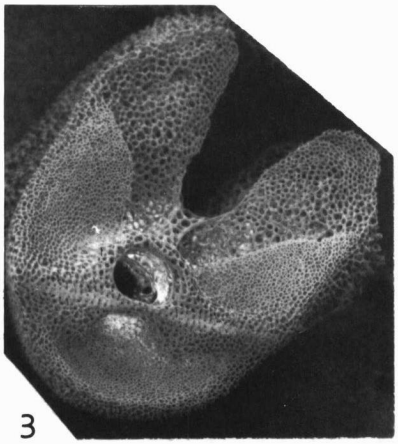
3

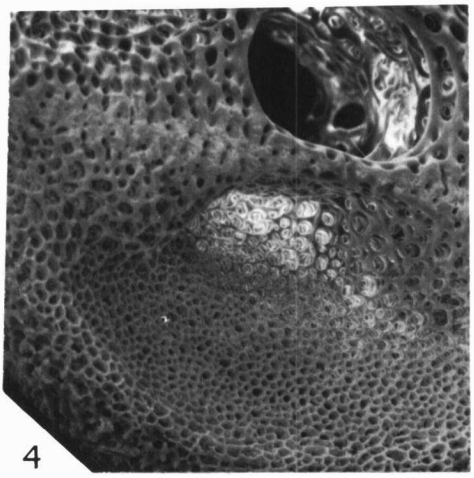
4

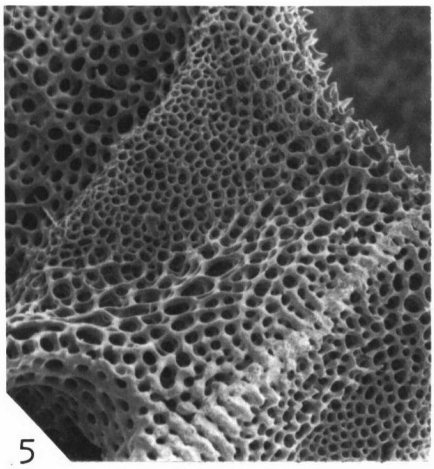
5

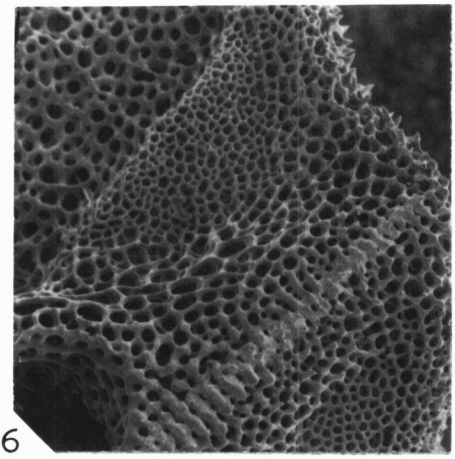
6

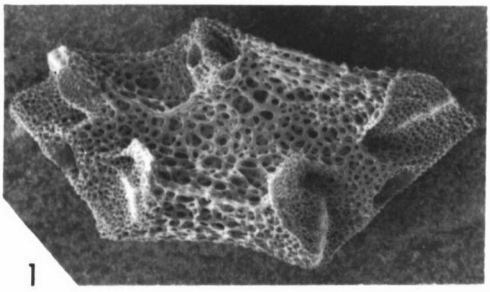
1

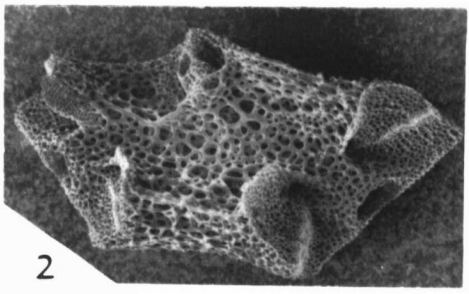
2

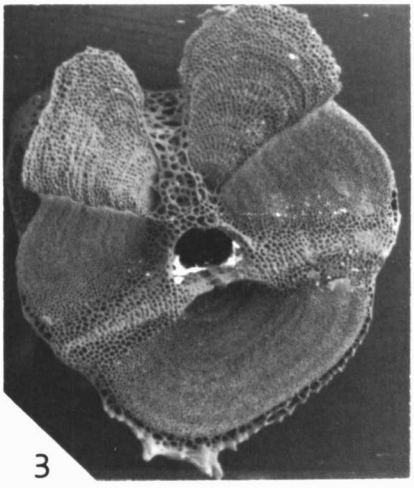
3

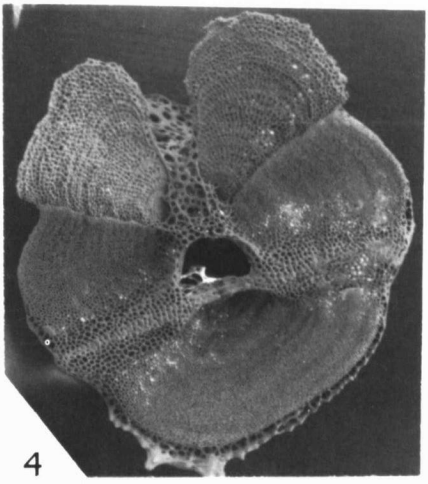
4

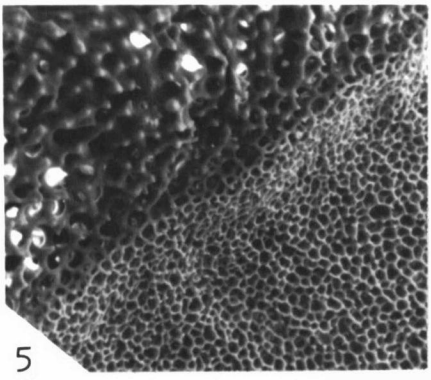
5

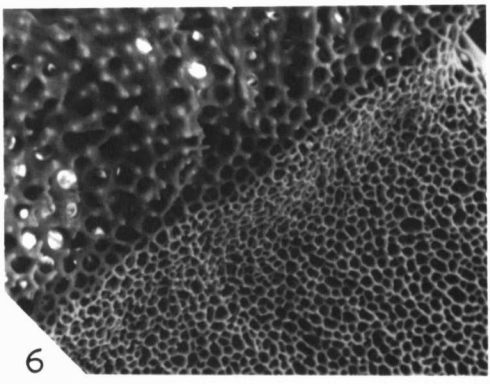
6

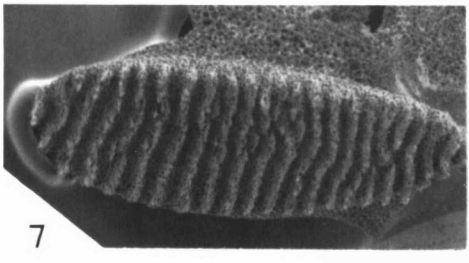
7

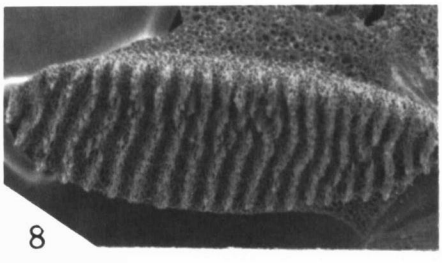
8

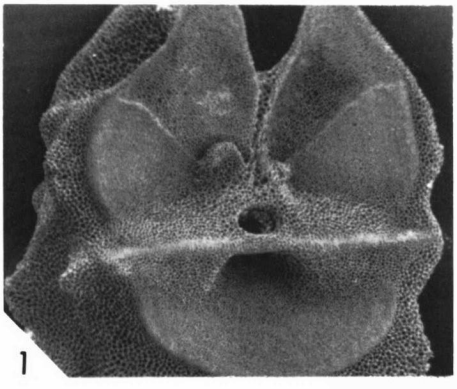
1

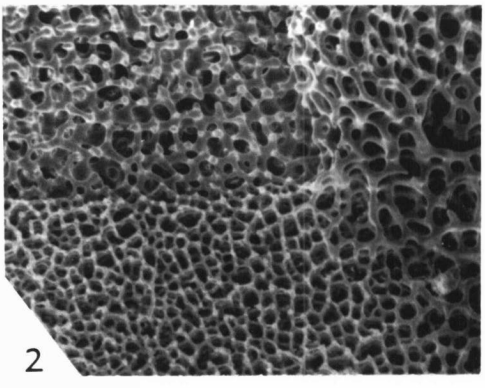
2

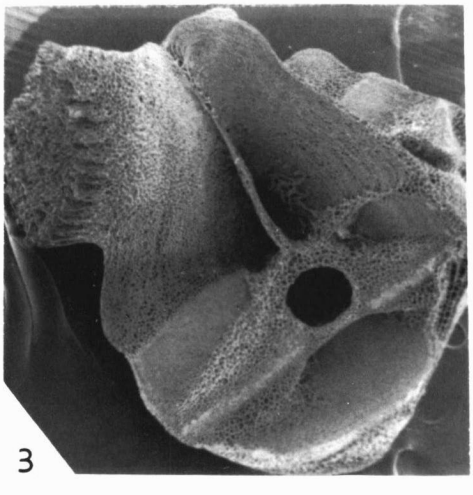
3

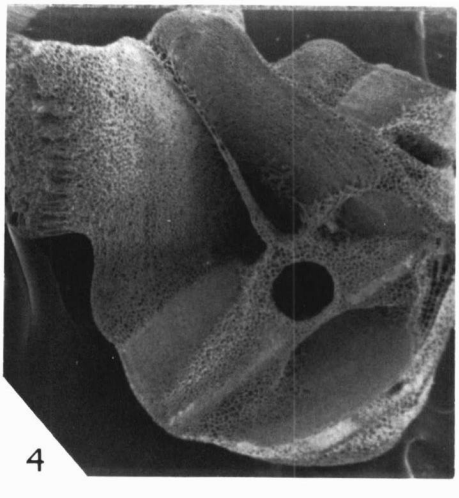
4

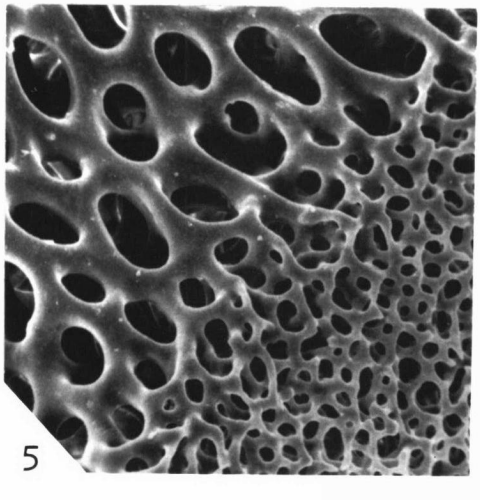
5

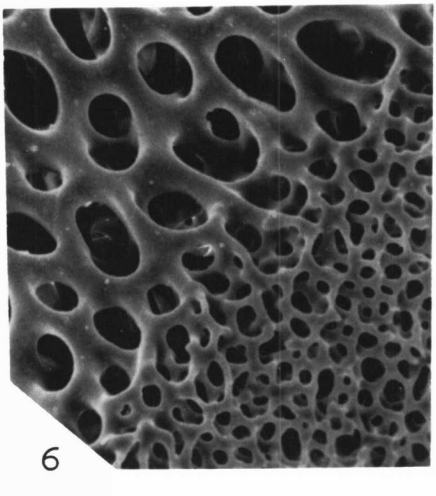
6

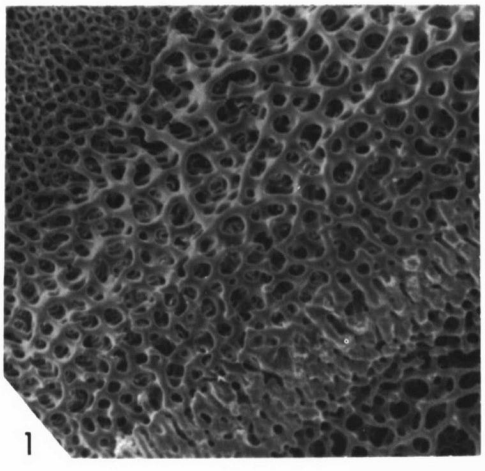
1

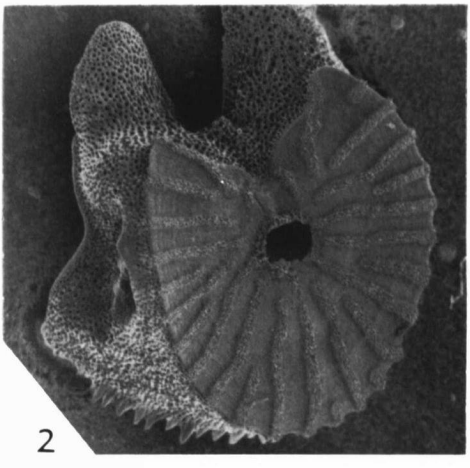
2

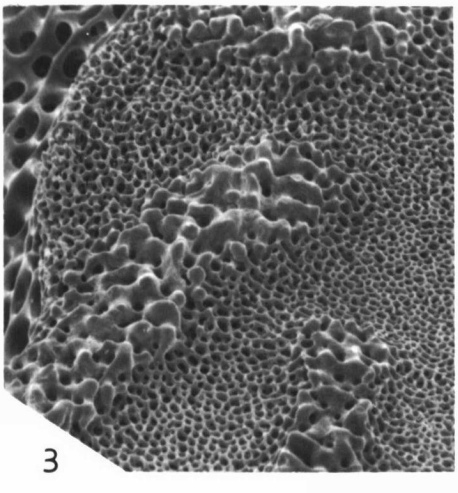
3

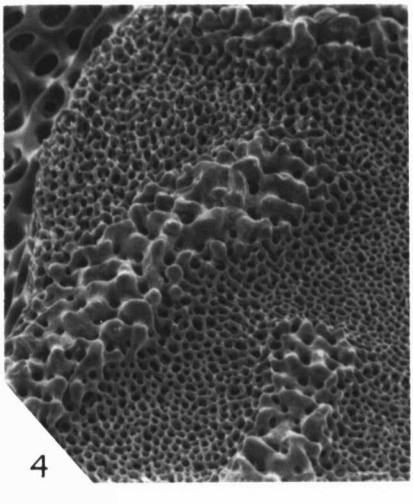
4

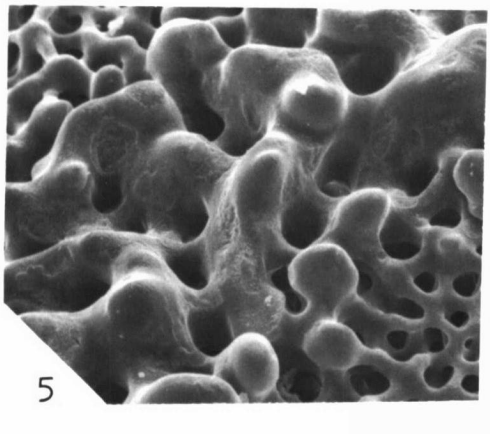
5

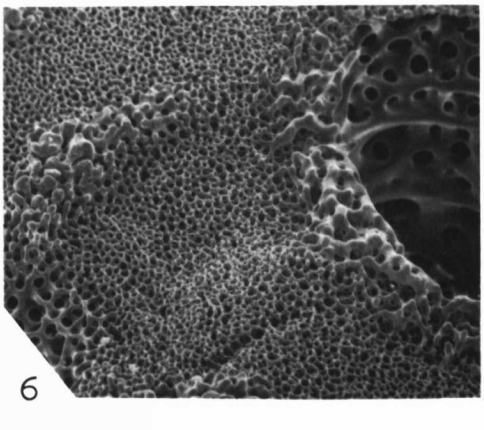
6

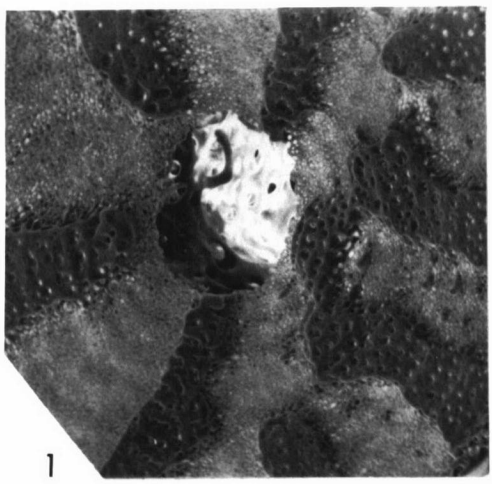
1


2

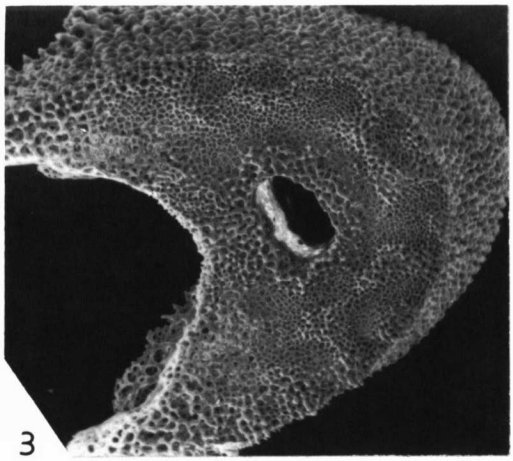
3

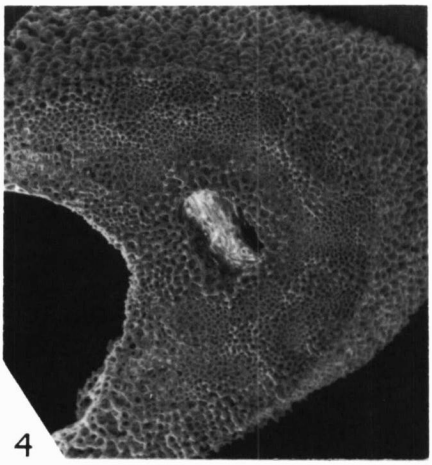
4

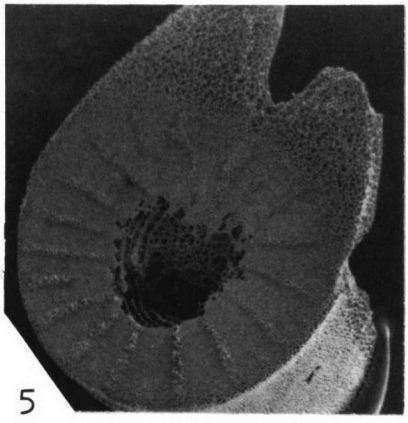
5

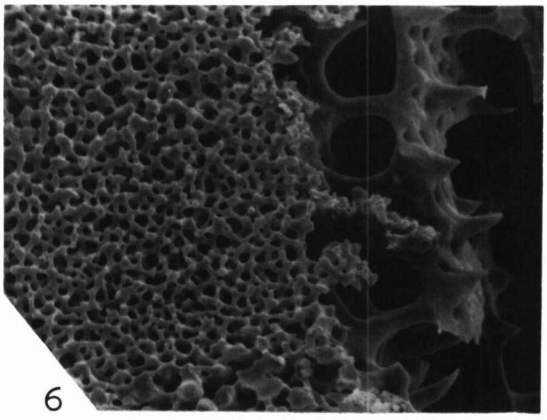
6

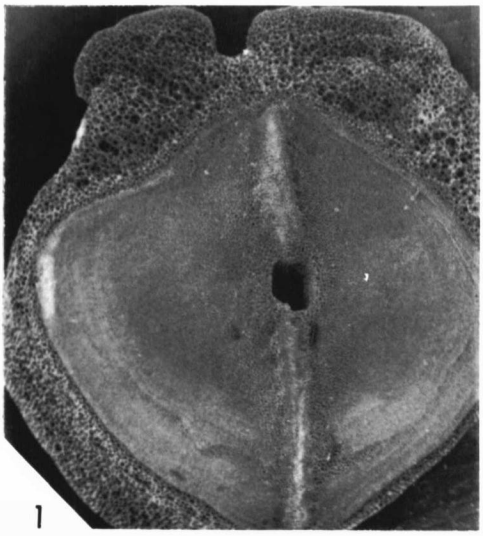

1

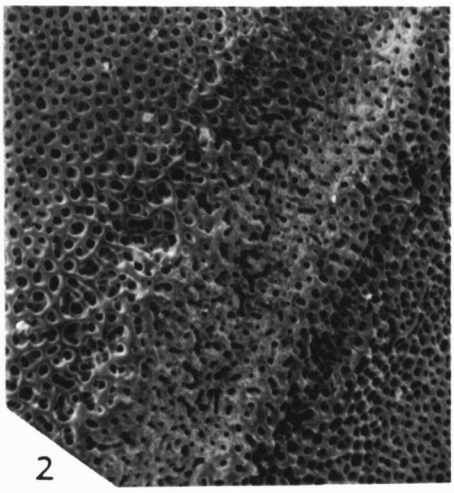

2

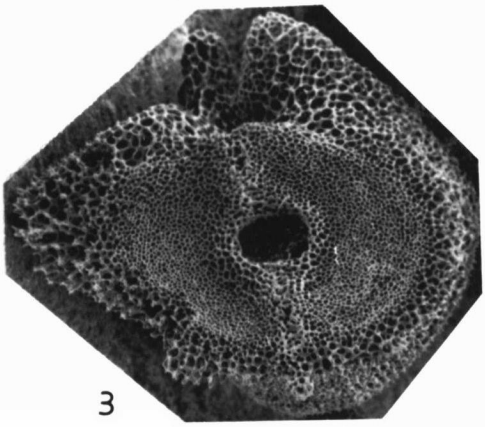

3

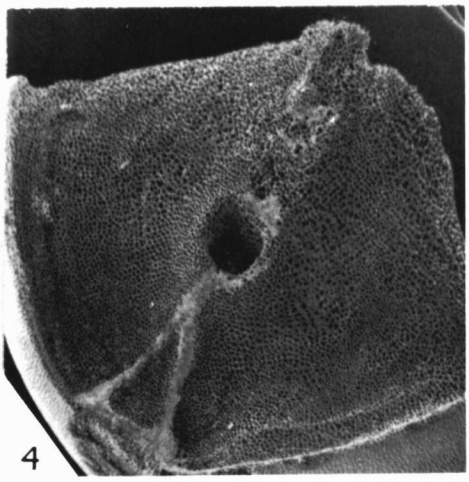

4

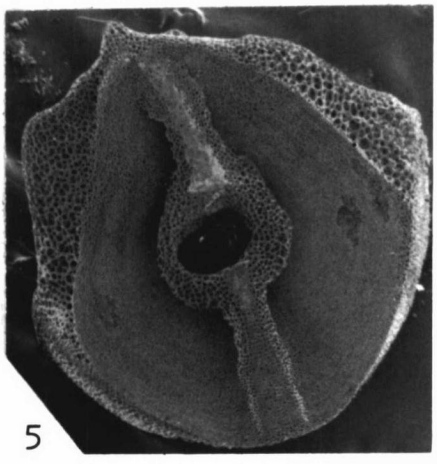

5

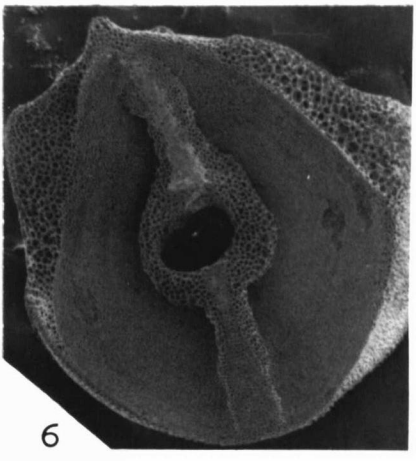

6

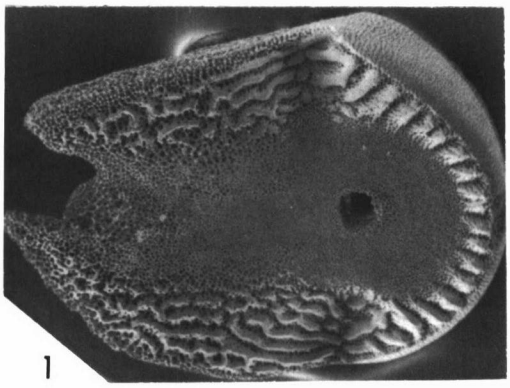
1

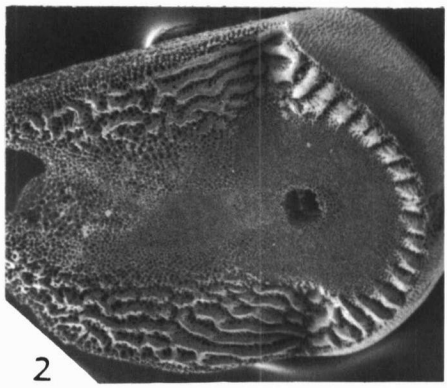
2

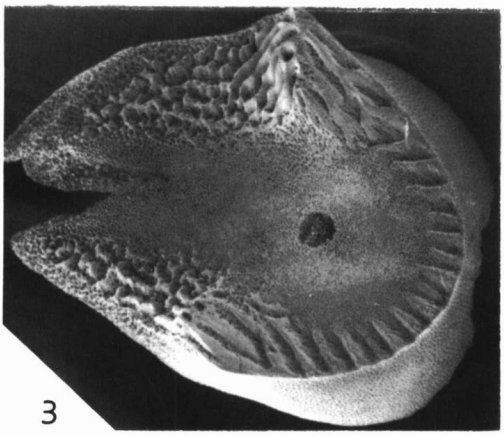
3

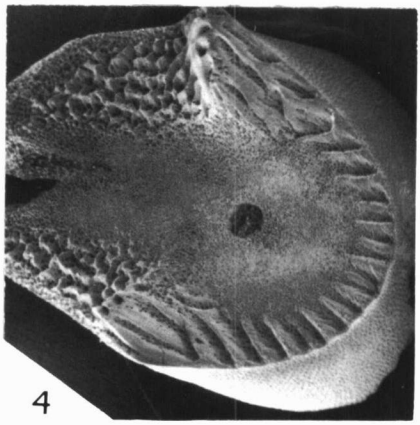
4

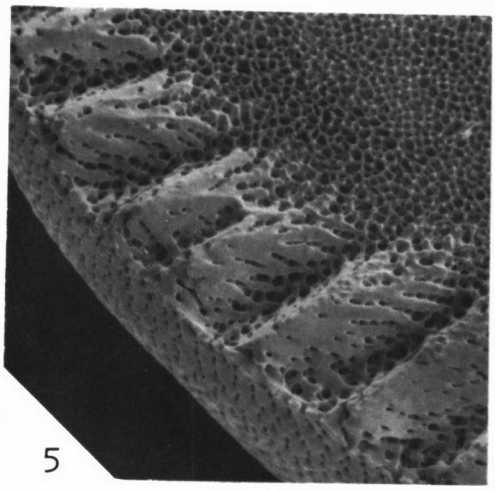
5

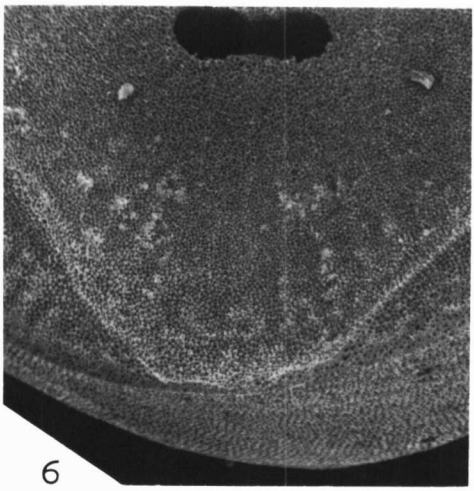
6

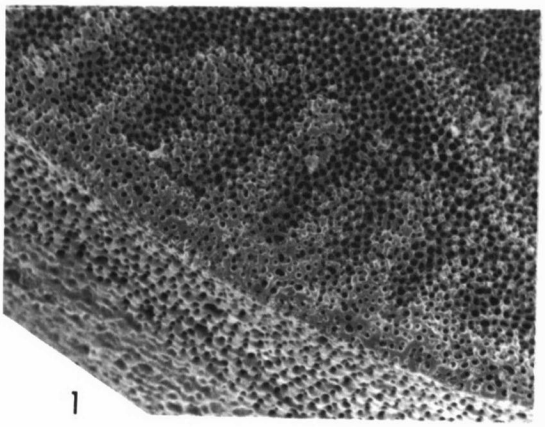
1

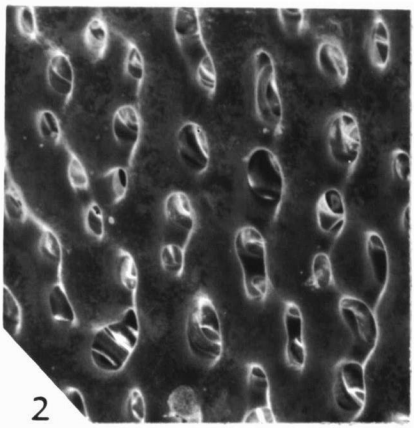
2

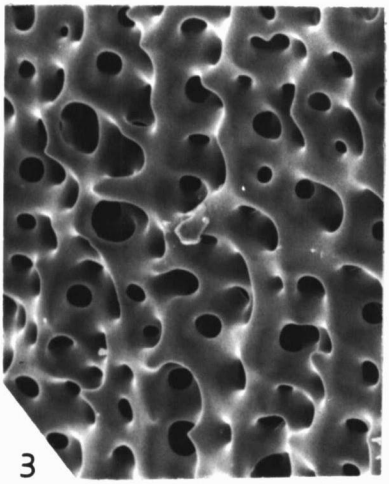
3

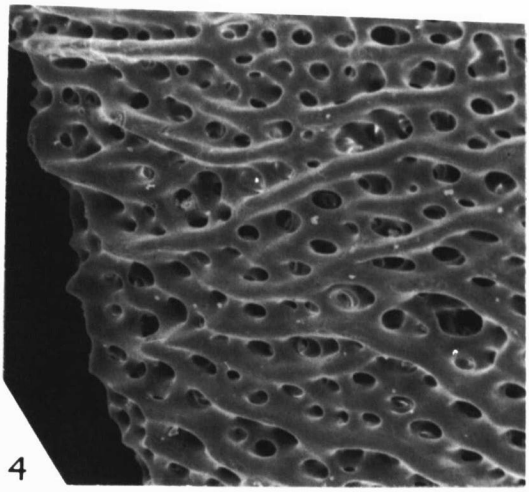
4

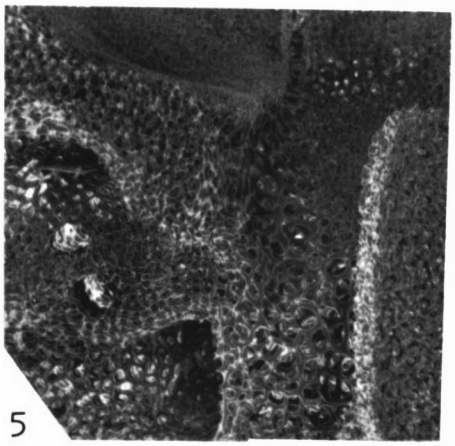
5

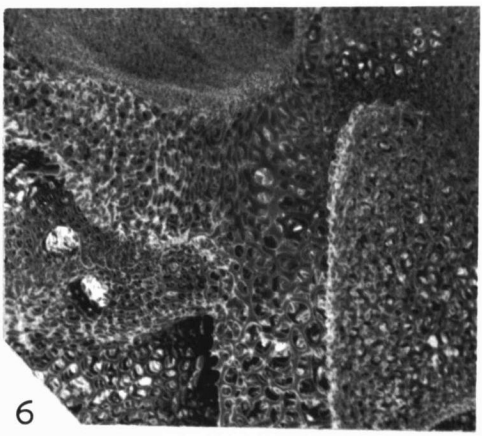
6

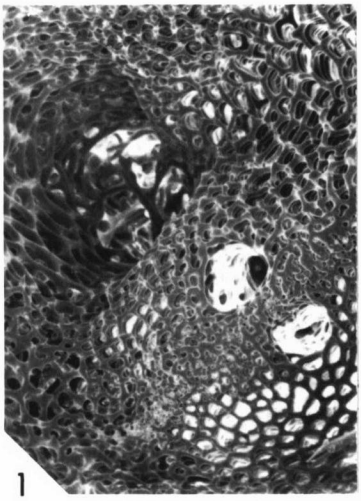
1

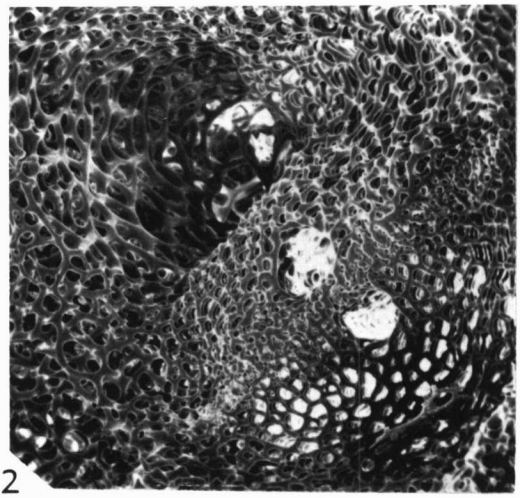
2

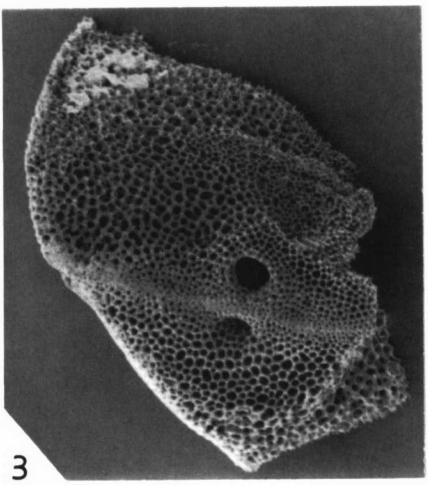
3

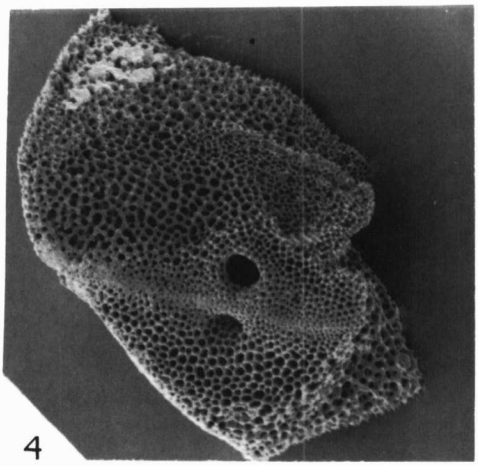
4

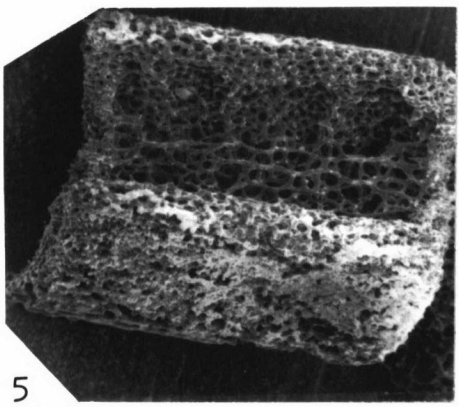
5

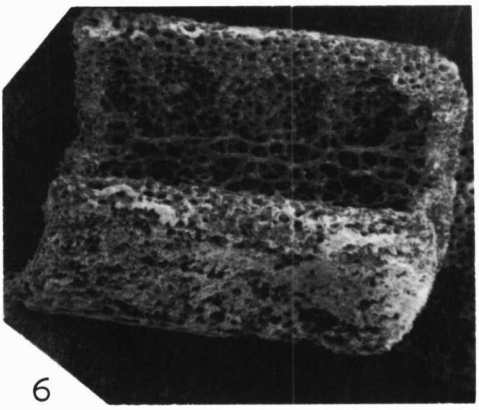
6

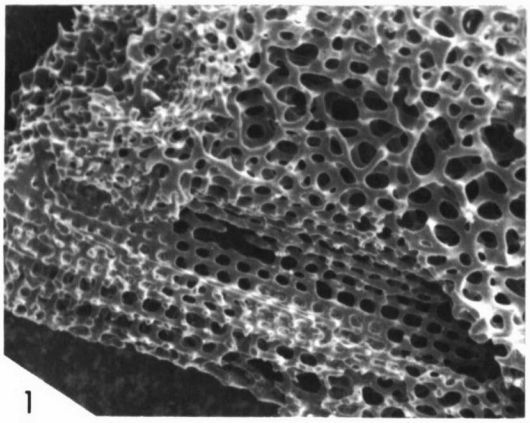
1

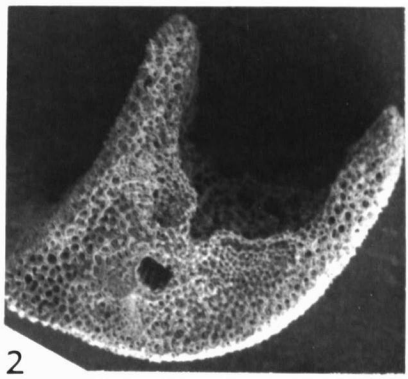
2

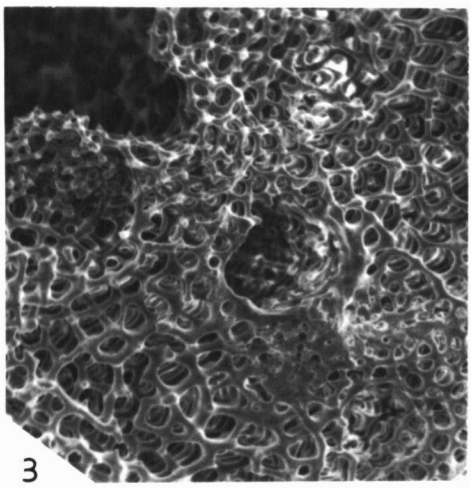
3

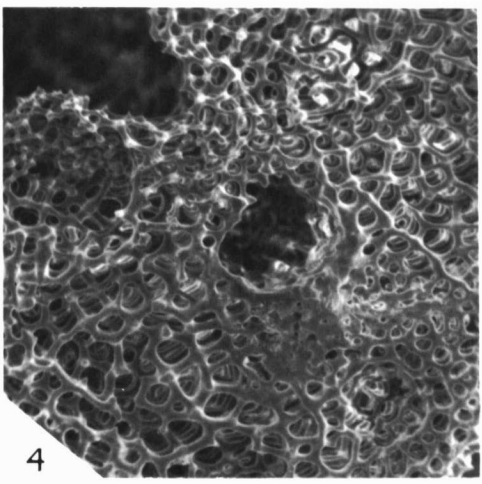
4

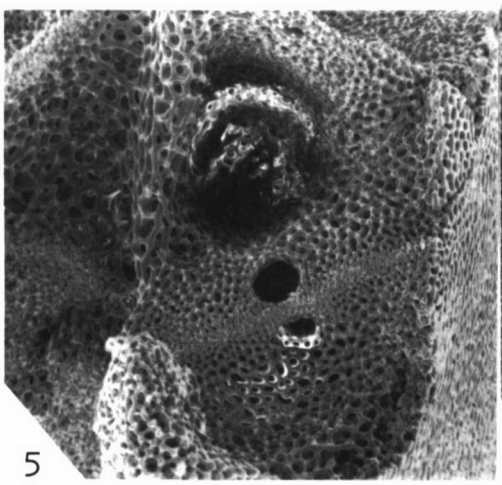
5

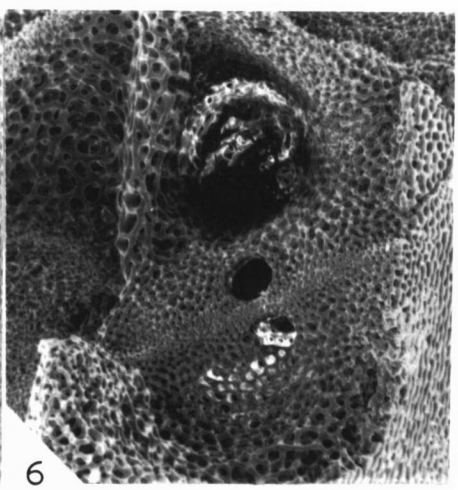
6

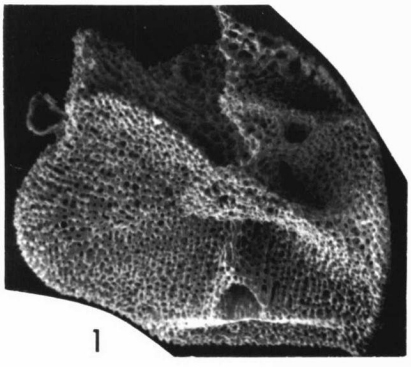
1

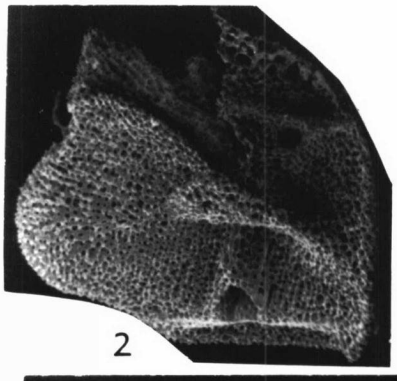
2

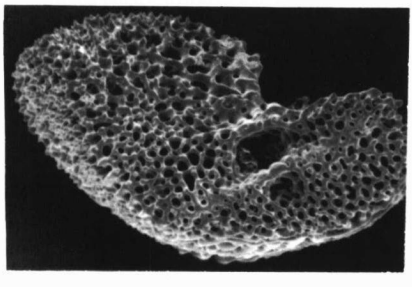
3

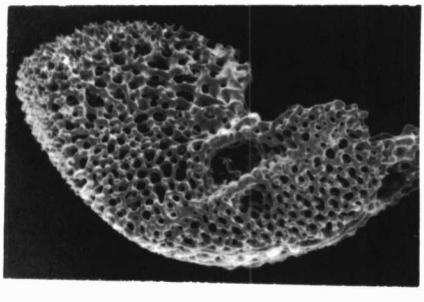
4

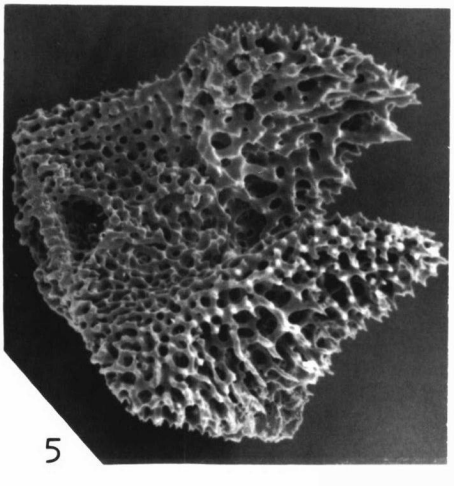
5

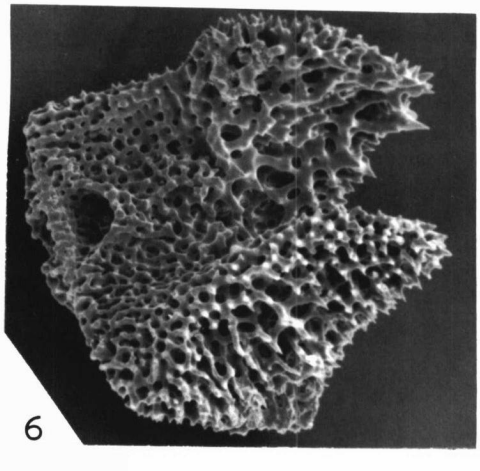
6

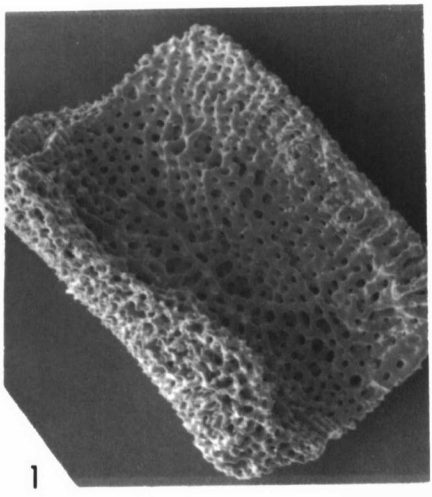
1

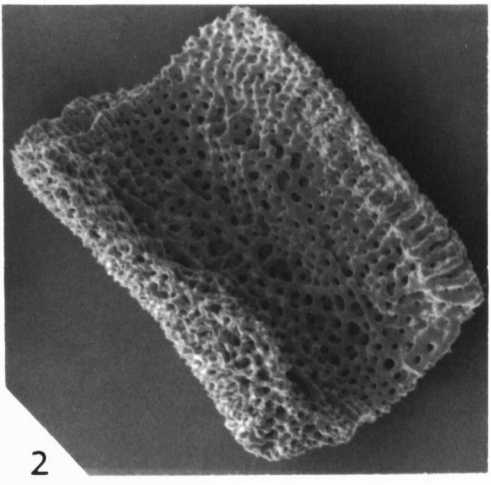
2

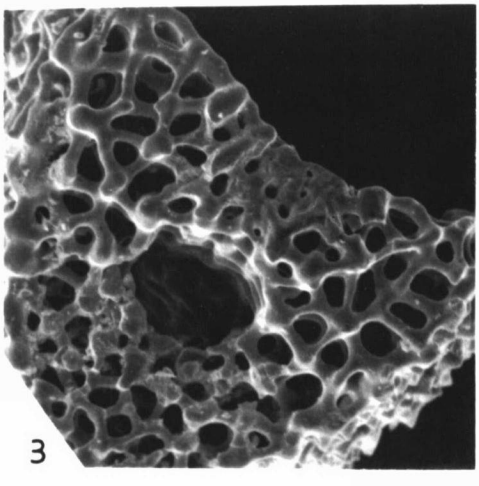
3

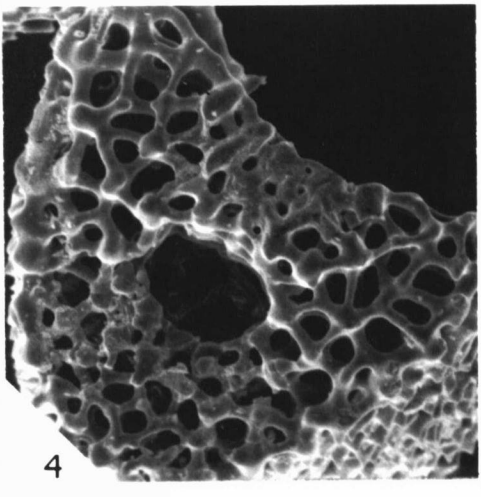
4

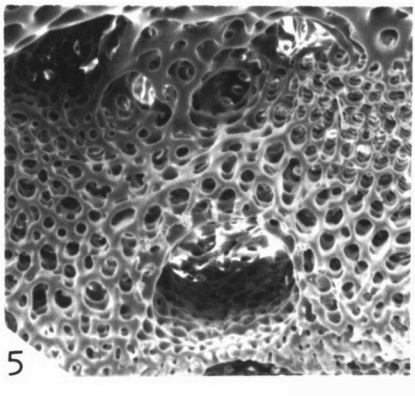
5

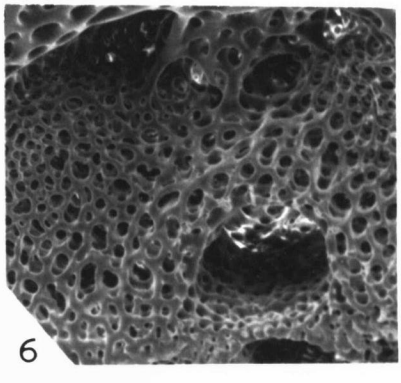
6

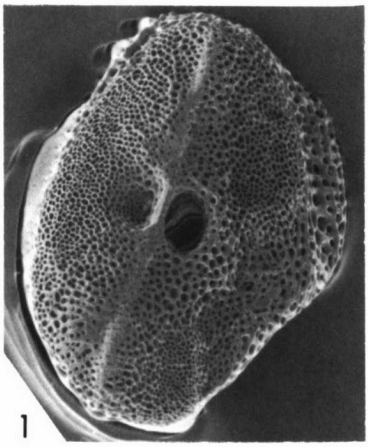
1

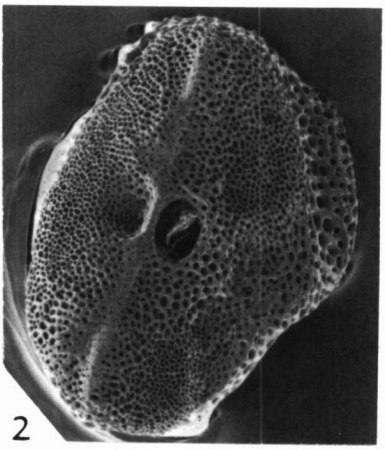
2


3

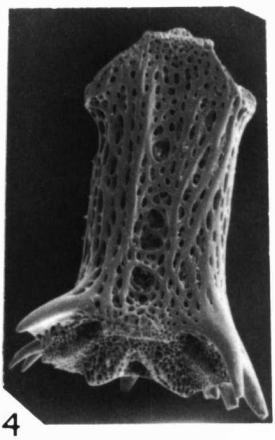
4

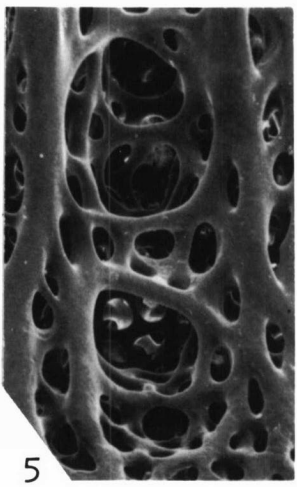
5

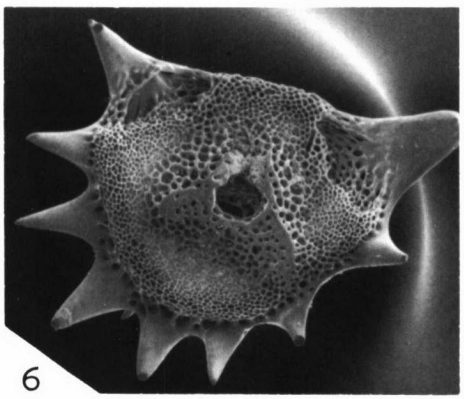
6

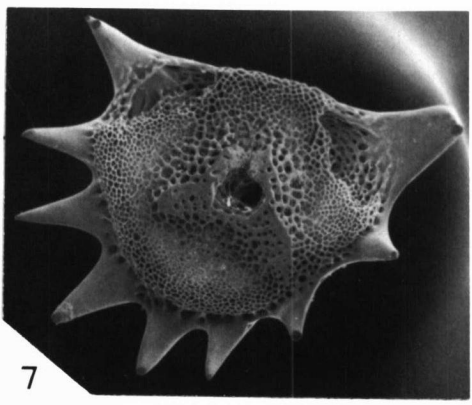
7

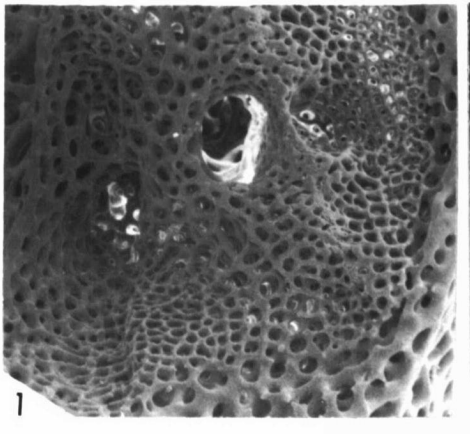
1

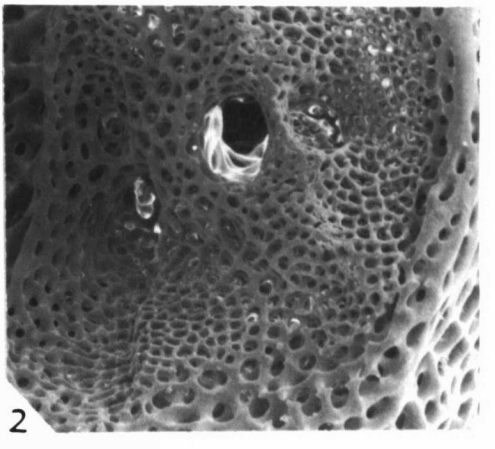
2

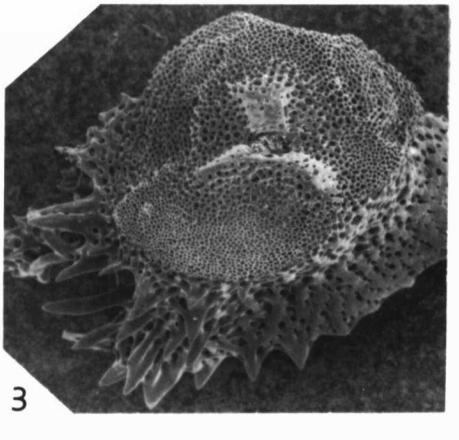
3

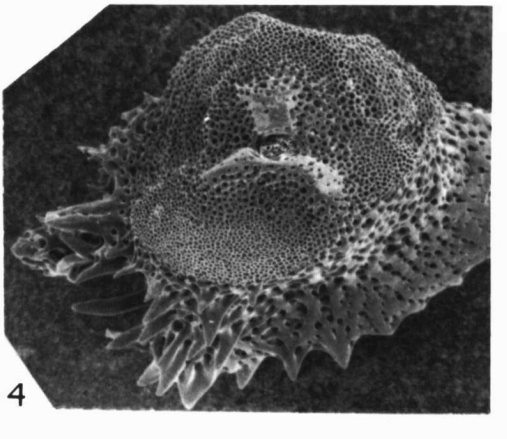
4

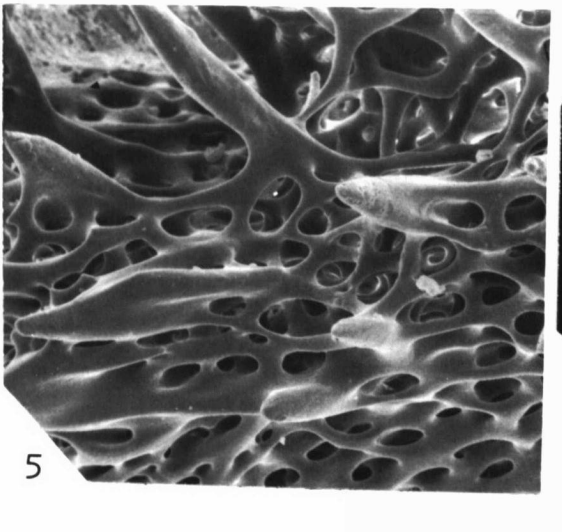
5

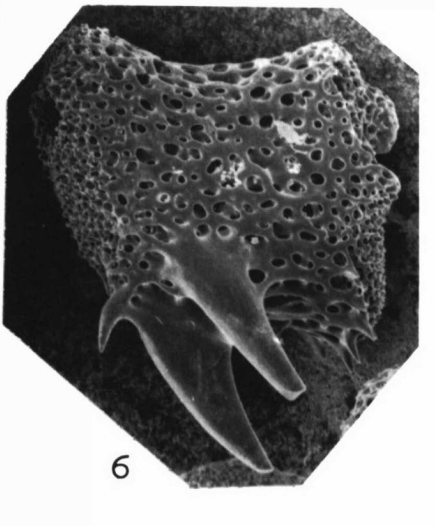
6

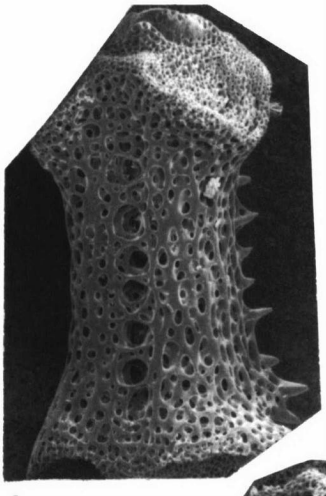

1

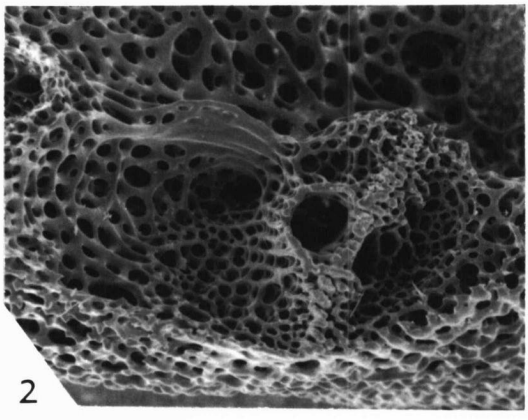

2

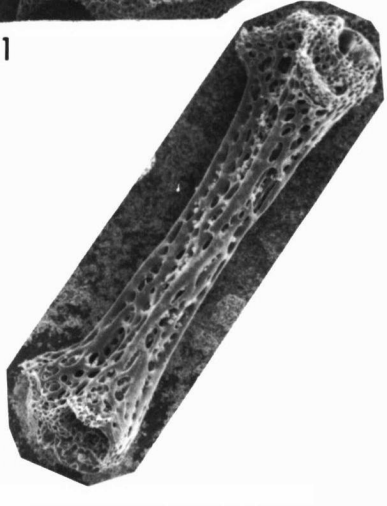

3

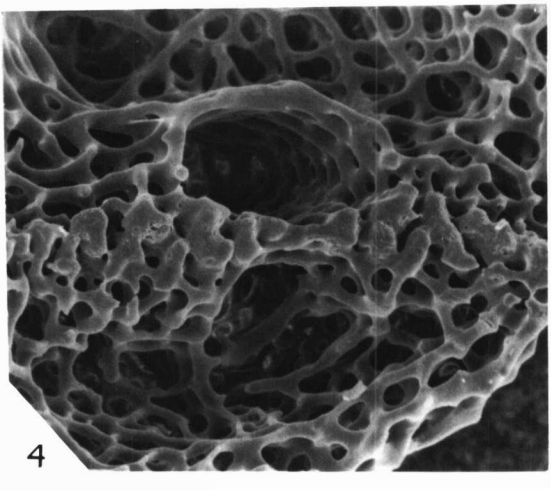

4

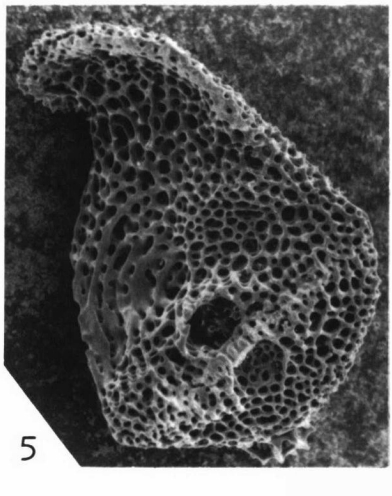

5

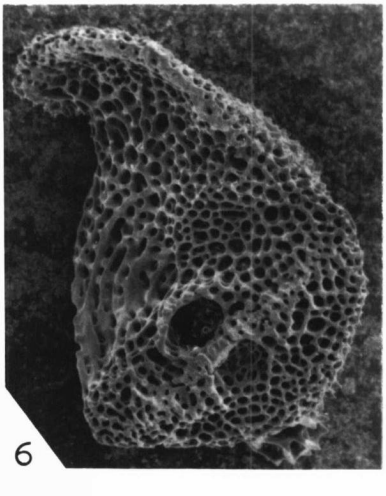

6